MODEL-DERIVED CHEMICAL-LOOPING SYSTEM DESIGNS

George M. Bollas

Department of Chemical & Biomolecular Engineering
University of Connecticut

http://pdsol.engr.uconn.edu

About

- **Diploma in Chemical Engineering**
  - Aristotle University of Thessaloniki – Greece
- **Ph.D. in Chemical Engineering**
  - Aristotle University of Thessaloniki – Greece
- **Postdoc in Chemical Engineering**
  - Massachusetts Institute of Technology – USA
- **Assistant Professor University of Connecticut**
  - NSF CAREER Award 2011
  - ACS-PRF DNI Award 2013
  - >$2M in research grants in 2010-2013
  - 9 graduate researchers
  - 10 undergraduate researchers

Research Group (PDSOL)

Enabling emerging energy technologies via integration of modeling with experimentation of processes lacking fundamental understanding

Catalysis for renewable fuels

- Novel spouted-bed reactor for biomass thermochemical processes (pyrolysis, gasification, chemical-looping combustion)
- Comprehensive catalyst characterization and catalyst activity dynamic simulation

Process Design, Scale-up & Control

- Dynamic simulation & optimization
  Optimal experimental design
- Model-assisted scale-up based on dynamic sensitivity analysis
- Chemical-looping combustion & reforming

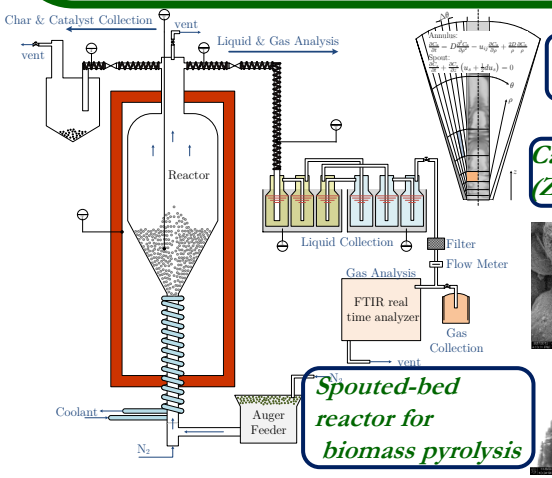

Dynamic simulation of a spouted bed

Catalyst characterization (ZSM-5 after pyrolysis)

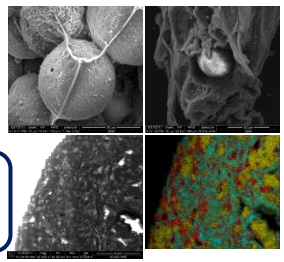

Spouted-bed reactor for biomass pyrolysis

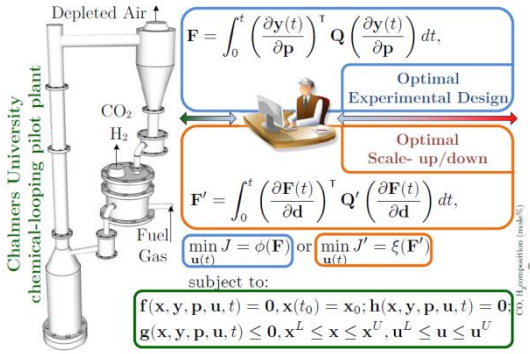

Fixed-bed reactor developed and simulated in PDSOL. Application of Optimal Experimental Design on the laboratory reactor. Scale-up based on sensitivity analysis of the bench-scale reactor.

Climate change urgency

- Carbon capture needs to be deployed to effectively lower the global CO_2 portfolio

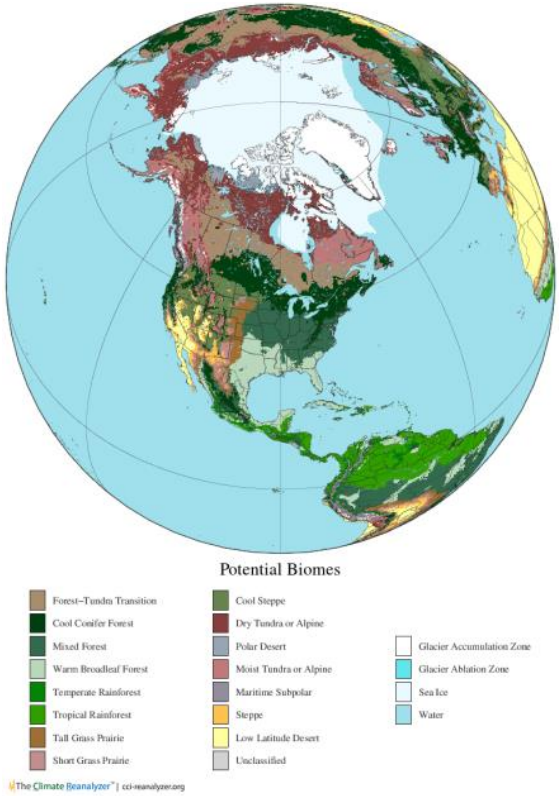

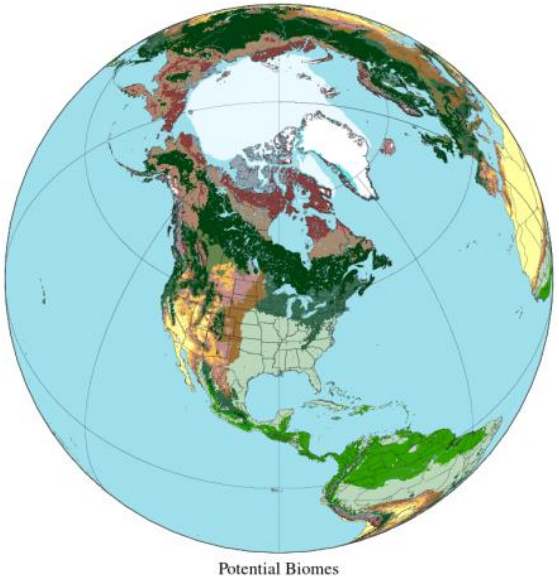

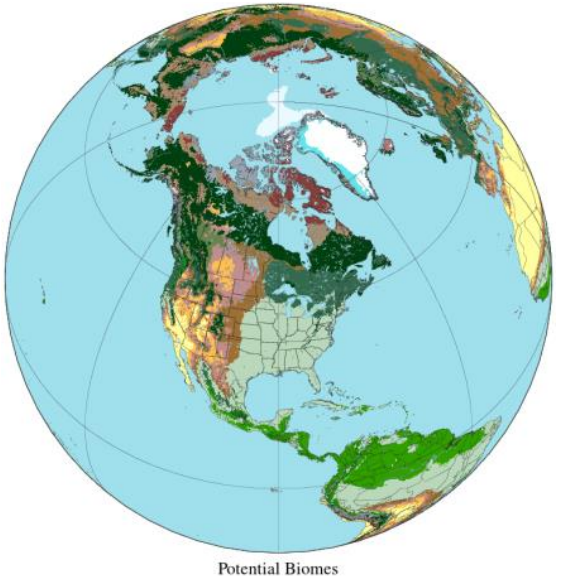

Fig.1: *University of Maine Environmental Change Model (UM-ECM) potential biomes calculated for modern climate. From left to right: input cooled by 4°C; todays input; input warmed by 2.5°C. Note the effect on the arctic sea ice. Data/images obtained using Climate Reanalyzer™ (http://cci-reanalyzer.org), Climate Change Institute, University of Maine, USA.*

US-wide CO_2 storage capacity

- Estimated total storage capacity of over 100 Gt in the continental US

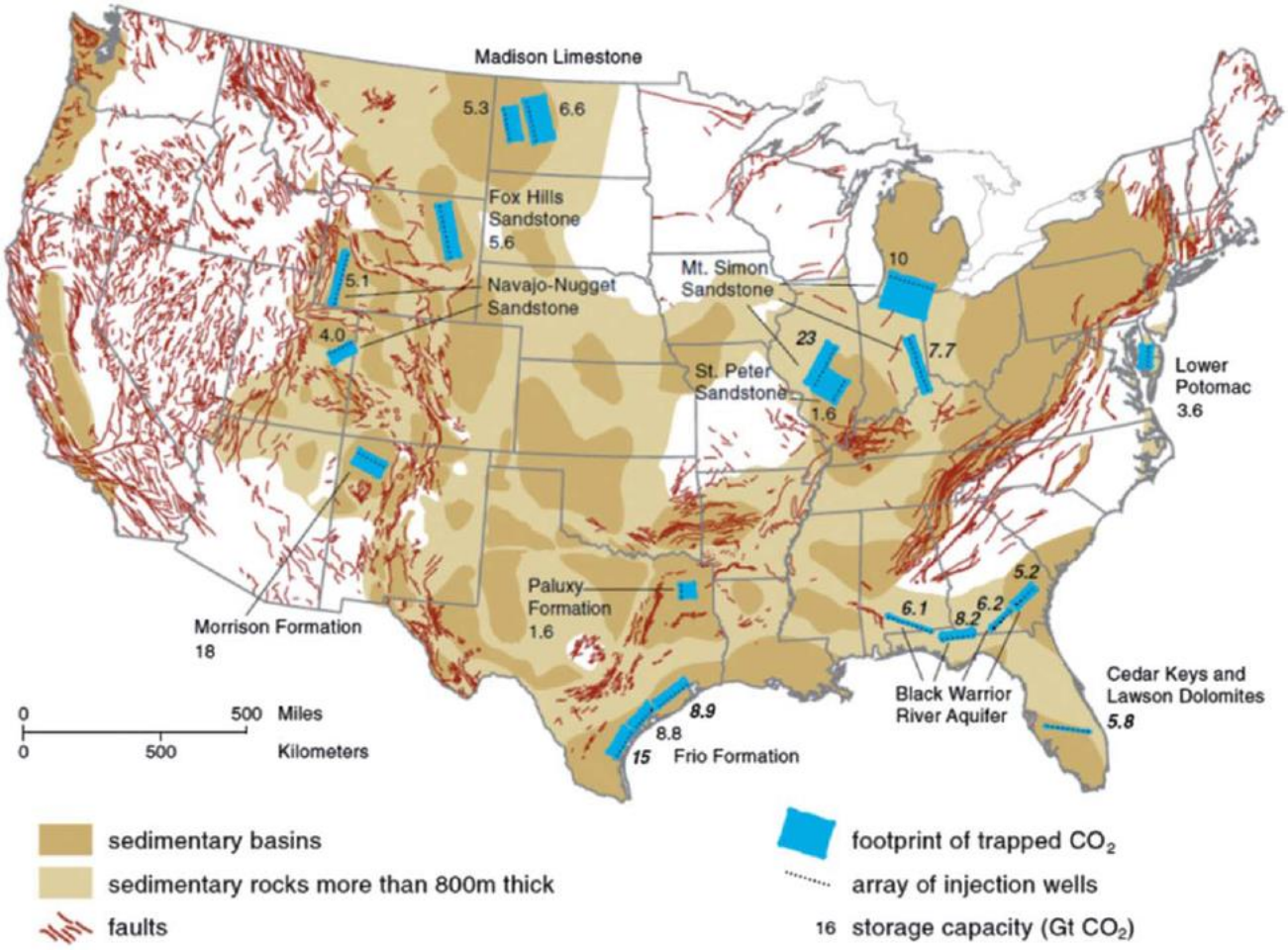

CO_2 Capture Options

- **Back in 2008**

Resource: America's Energy Future Technology And Transformation, *Committee On America's Energy Future, National Academy Of Sciences, National Academy of Engineering, National Research Council of The National Academies,* The National Academies Press

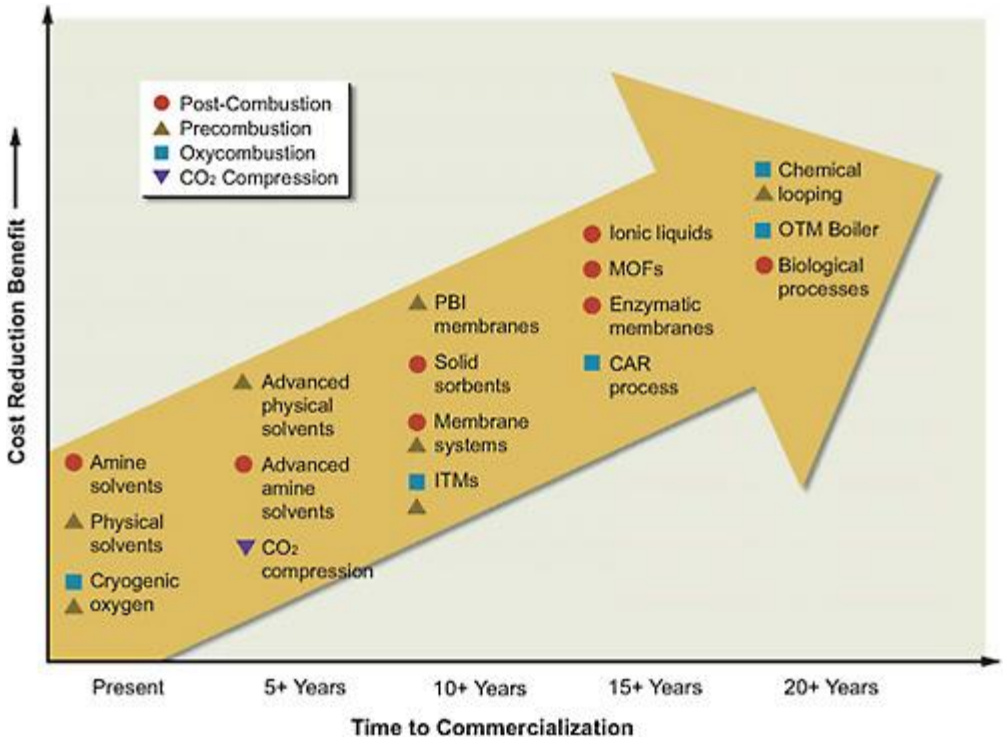

Chemical-looping progress

- Boot-Handford ME, Abanades JC, Anthony EJ, Blunt MJ, Brandani S, Mac Dowell N, et al. Carbon capture and storage update. Energy Environ Sci 2014.

Table 4 Testing in chemical-looping combustors[a]

Location	Unit	Oxides tested	Time	Fuel\references	Year
Chalmers	10 kW	NiO, Fe_2O_3	1410	Nat. gas\[575–578]	2004
KIER	50 kW	NiO, CoO	28	Nat. gas\[579,580]	2004
CSIC	10 kW	CuO, NiO	120	Nat. gas\[581,582]	2006
Chalmers	0.3 kW	NiO, Mn_3O_4, Fe_2O_3, ilmenite, $CaMnO_3$	810	Nat. gas, syngas\[227,241,583–591]	2006
Chalmers	10 kW-SF	Ilmenite, manganese ore	149	Coal, petcoke\[245,259,592–595]	2008
CSIC	0.5 kW	CuO, NiO, Fe_2O_3	820	Nat. gas\[228,254,596–606]	2009
KAIST	1 kW	NiO + Fe_2O_3	?	CH_4\[607]	2009
Vienna UT	140 kW	Ilmenite, NiO	390	Nat. gas, CO, H_2\[262,608–617]	2009
Alstom	15 kW	NiO	100	Nat. gas\[4]	2009
Nanjing	10 kW-SF	NiO, Fe_2O_3	230	Coal, biom.\[618–621]	2009
KIER	50 kW	NiO, CoO	300	Nat. gas, syngas\[622]	2010
Nanjing	1 kW-SF	Fe_2O_3 (ore)	>10	Coal, biomass\[244,623]	2010
IFP-Lyon	10 kW-GSF	NiO	>90	CH_4, coal, syngas\[624,625]	2010
Stuttgart	10 kW	Ilmenite	?	Syngas\[261]	2010
Xi'an Jiaotong	10 kW-Pr	CuO/Fe_2O_3	15	Coke oven gas\[626]	2010
CSIC	0.5 kW-SF	Ilmenite, CuO, Fe_2O_3	164	Coal\[260,265,627,628]	2011
Chalmers	0.3 kW-LF	NiO, Mn_3O_4, CuO	116	Kerosene\[214,215]	2011
Chalmers	100 kW-SF	Ilmenite	24	Coal\[629–632]	2012
Hamburg	25 kW-SF	Ilmenite	21	Coal\[633]	2012
Ohio	25 kW-SF	Fe_2O_3	~72	Coal\[634]	2012

[a] SF – solid fuel, GSF – gaseous & solid fuel, Pr – pressurised, LF – liquid fuel.

Chemical-looping combustion (CLC)

- **A method for inherent CO_2 separation**
  - **Oxygen carriers**
    - **M : metal**
    - **MO : metal oxide**

Reduction: endothermic

$$CH_4 + 4MO \rightarrow CO_2 + 2H_2O + 4M$$

Oxidation: exothermic

$$M + \tfrac{1}{2} O_2 \rightarrow MO$$

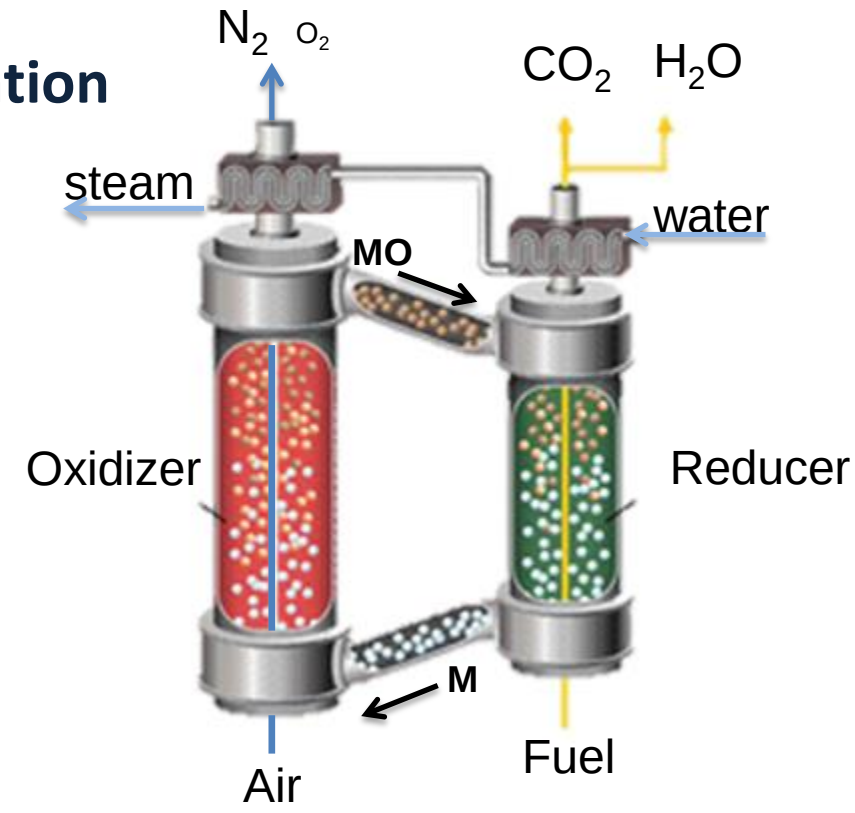

- Circulating oxygen carrier: active metal oxides (Ni, Cu, Fe, Mn) supported over Al_2O_3, $MgAl_2O_4$, $NiAl_2O_4$, YSZ, TiO_2, ZrO_2.
- Reactivity testing: TGA, fixed-bed, interconnected fluidized-beds.

Our work

- **[1] Zhou Z, Han L, Bollas GM. Model-based analysis of bench-scale fixed-bed units for chemical-looping combustion. Chem Eng J 2013;233:331–48.**
- **[2] Han L, Zhou Z, Bollas GM. Heterogeneous Modeling of Chemical-Looping Combustion. Part 1: Reactor Model. Chem Eng Sci 2013;104:233 – 249.**
- [3] Han L, Zhou Z, Bollas GM. Heterogeneous Modeling of Chemical-Looping Combustion. Part 2: Particle Model. Chem Eng Sci 2014;in press.
- **[4] Zhou Z. Han L, Bollas GM. Overview of Chemical-Looping Reduction in Fixed Bed and Fluidized Bed Reactors Focused on Oxygen Carrier Utilization and Reactor Efficiency. Aerosol Air Qual Res 2014;14:559–71.**
- [5] Zhou Z, Han L, Bollas GM. Kinetics of NiO reduction by H_2 and Ni oxidation at conditions relevant to chemical-looping combustion and reforming. Int J Hydrogen Energy 2014;in press.
- ***[6] Han L, Zhou Z, Bollas GM. Chemical-looping combustion in a reverse-flow fixed-bed reactor. Appl Energy 2014;in review.***
- **[7] Zhou Z, Han L, Bollas GM. Model-assisted analysis of fluidized bed chemical-looping reactors. AIChE J 2014;in review.**
- **[8] Han L, Zhou Z, Bollas GM. Optimal Experimental Design for Fixed Bed Chemical-Looping Experiments. Comput Chem Eng 2014;in preparation.**

The "dream concept"

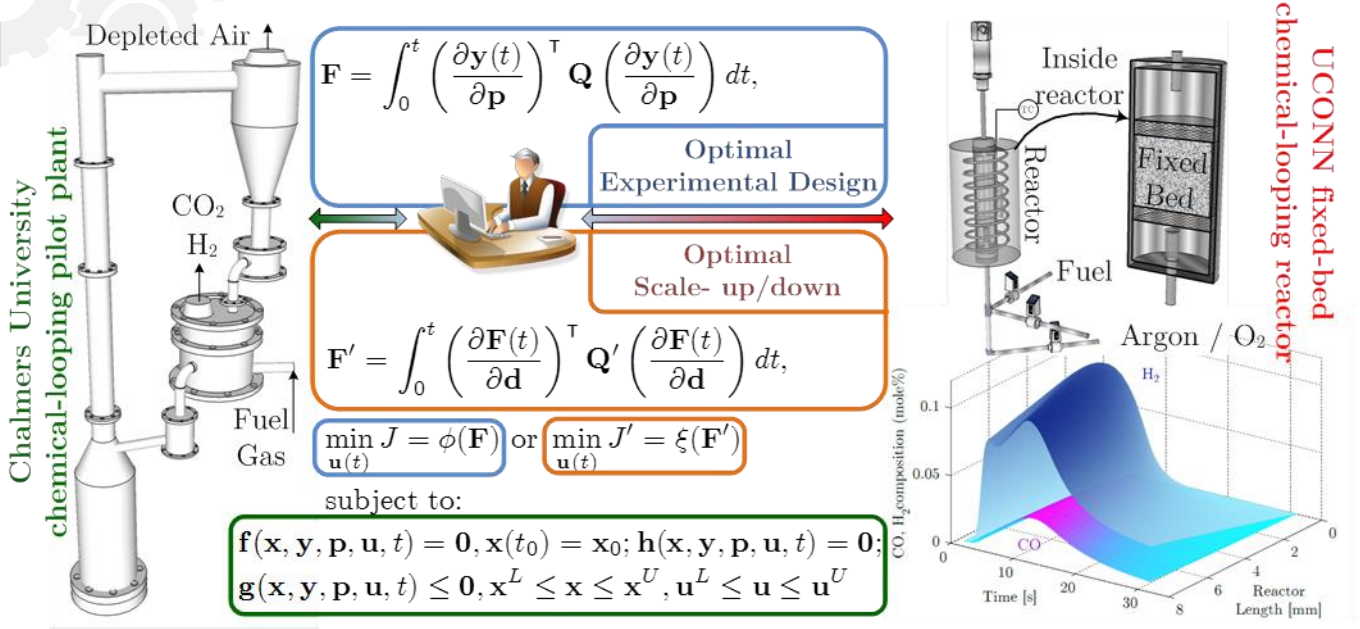

- maximize information content of experiments
- integrate experimentation with reactor design
- obtain scale-independent process models
- estimate model parameters that increase the accuracy of process scale-up/scale-down
- reduce risk of technology scale-up/scale-down.

- **<u>OED for process scaling of chemical-looping</u>:**
  Measurements of bench- and pilot- scale processes are used to develop state/space models. These models are subsequently used to identify time-varying experimental conditions that maximize the statistical significance of the measurements with respect to process scale, subject to constraints.

Fixed-bed model description

Heterogeneous model

Fluid phase

$$\varepsilon_b \frac{\partial C_i}{\partial t} + \frac{\partial F_i}{\partial V} = \frac{\partial}{\partial z}\left(\varepsilon_b D_{ax,i} \frac{\partial C_i}{\partial z}\right) + k_{c,i} a_v \left(C_{c,i}|_{R_p} - C_i\right)$$

$$\varepsilon_b Cp_f C_T \frac{\partial T}{\partial t} + Cp_f F_T \frac{\partial T}{\partial V} = \frac{\partial}{\partial z}\left(\varepsilon_b \lambda_{ax} \frac{\partial T}{\partial z}\right)$$

$$+ h_f a_v \left(T_c|_{R_p} - T\right) + \frac{4U}{DR}(T_w - T)$$

Solid phase

$$\varepsilon_c \frac{\partial C_{c,i}}{\partial t} = \frac{1}{{r_c}^2} \frac{\partial}{\partial r_c}\left(D_{e,i} {r_c}^2 \frac{\partial C_{c,i}}{\partial r_c}\right) + \rho_s \sum R_i$$

$$\left((1-\varepsilon_c)\,\rho_s Cp_s + \varepsilon_c Cp_c C_{T,c}\right)\frac{\partial T_c}{\partial t} =$$

$$\frac{\lambda_s}{{r_c}^2}\frac{\partial}{\partial r}\left({r_c}^2 \frac{\partial T_c}{\partial r_c}\right) + \rho_s \sum(-\Delta H_i)(R_i)$$

Pressure drop

$$\frac{dP}{dz} = -\left(\frac{1-\varepsilon_b}{{\varepsilon_b}^3}\right)\left(\frac{\rho u_0^2}{D_p}\right)\left(\frac{150}{Re_p} + 1.75\right)$$

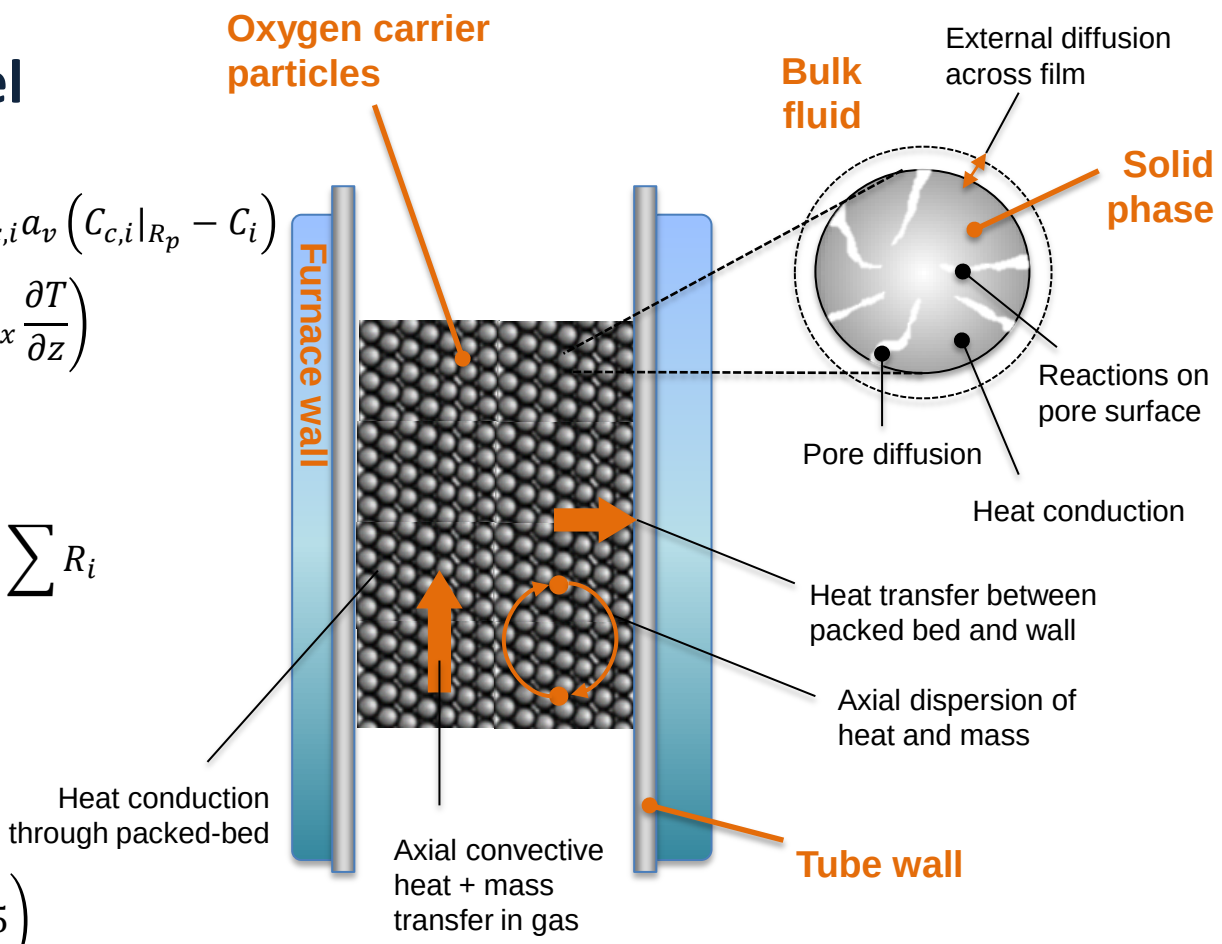

Han, L.; Zhou, Z.; Bollas, G. M. Heterogeneous Modeling of Chemical-Looping Combustion. Part 1: Reactor Model. *Chemical Engineering Science* 2013

Fixed-bed model application

- Application to experimental data of CLC by Iliuta et al. (2010), Ryden et al. (2008) and CLR data by Jin (2002)

Han, L.; Zhou, Z.; Bollas, G. M. Heterogeneous Modeling of Chemical-Looping Combustion. Part 1: Reactor Model. *Chemical Engineering Science* **2013**

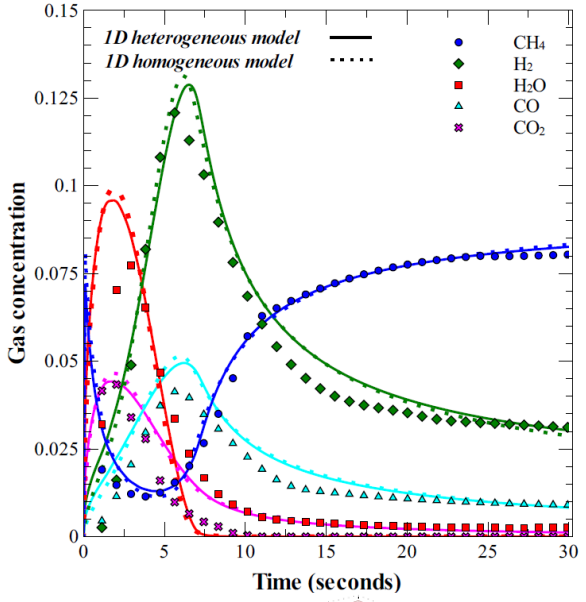

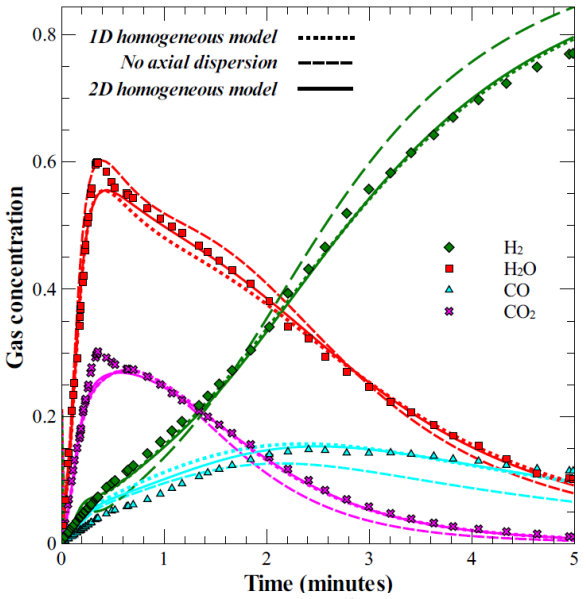

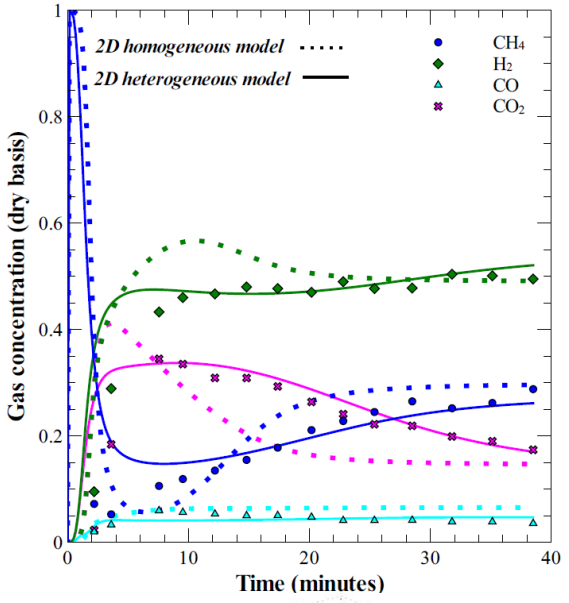

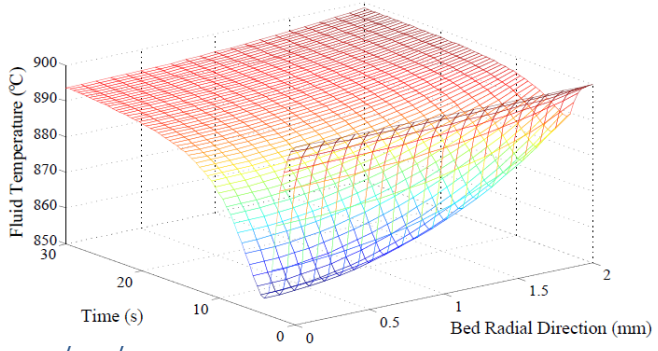

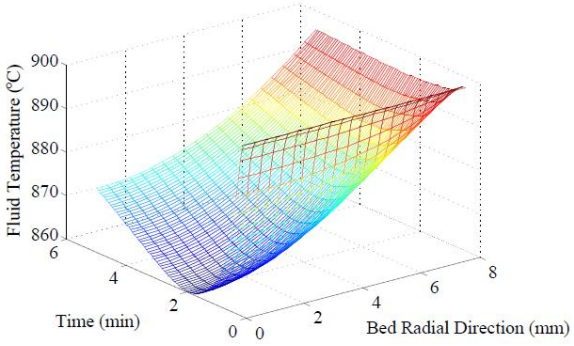

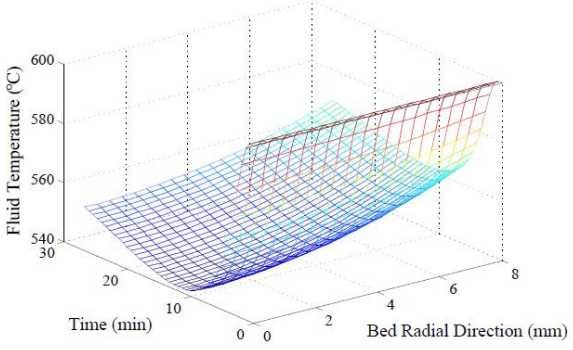

Reduction reactions with NiO

Oxygen carrier reduction reactions	CH_4 oxidation	$CH_4 + 2NiO \leftrightarrow 2Ni + CO_2 + 2H_2$	ΔH° = 165 kJ/mol
	H_2 oxidation	$H_2 + NiO \leftrightarrow Ni + H_2O$	ΔH° = -2.2 kJ/mol
	CO oxidation	$CO + NiO \leftrightarrow Ni + CO_2$	ΔH° = -43.3 kJ/mol
	Partial CH_4 oxidation	$CH_4 + NiO \leftrightarrow Ni + 2H_2 + CO$	ΔH° = 203 kJ/mol
Reactions catalyzed by Ni	Steam reforming	$CH_4 + H_2O \leftrightarrow 3H_2 + CO$	ΔH° = 205 kJ/mol
	Water gas shift	$CO + H_2O \leftrightarrow H_2 + CO_2$	ΔH° = -41.1 kJ/mol
	Dry reforming	$CH_4 + CO_2 \leftrightarrow 2CO + 2H_2$	ΔH° = 247 kJ/mol
	Methane decomposition	$CH_4 \leftrightarrow 2H_2 + C$	ΔH° = 88 kJ/mol
	Carbon gasification by steam	$C + H_2O \leftrightarrow CO + H_2$	ΔH° = 131 kJ/mol
	Carbon gasification by CO_2	$C + CO_2 \leftrightarrow 2CO$	ΔH° = 173 kJ/mol

Zhou, Z.; Han, L.; Bollas, G. M. Model-based Analysis of Bench-Scale Fixed-Bed Units for Chemical-Looping Combustion. *Chemical Engineering Journal* **2013**

TGA Model

- **Mass balance**

$$\varepsilon_c \frac{\partial C_{c,i}}{\partial t} + \frac{1}{r_c^2}\frac{\partial}{\partial r_c}\left(r_c^2 v_c C_{c,i}\right) = \frac{1}{r_c^2}\frac{\partial}{\partial r_c}\left(r_c^2 \frac{\partial}{\partial r_c}\left(D_{\text{eff},i} C_{c,i}\right)\right) + \rho_s \sum R_j$$

- **Intraparticle velocity (forced convection)**

$$\frac{\partial v_c}{\partial r_c} = \frac{\sum_{j=1} R_j}{\sum_{i=1} C_{c,i}}$$

  - Boundary Conditions

$$-\frac{\partial\left(D_{\text{eff},i} C_{c,i}\right)}{\partial r_c}\bigg|_{r_c=r_p} + v_c\big|_{r_c=r_p} C_{c,i}\big|_{r_c=r_p} = k_{c,i}\left(C_{c,i}\big|_{r_c=r_p} - C_i\right) \qquad \frac{\partial C_{c,i}}{\partial r_c}\bigg|_{r_c=0} = v_c\big|_{r_c=0} = 0$$

- **Mass Balance around the crucible**

$$\varepsilon_b \frac{\partial C_i}{\partial t} = \varepsilon_b \frac{\partial}{\partial z}\left(D_{ax,i}\frac{\partial C_i}{\partial z}\right) + k_{c,i} a_v \left(C_{c,i}\big|_{r_c=r_p} - C_i\right)$$

  - Boundary Conditions

$$\varepsilon_b D_{ax,i}\left(\frac{\partial C_i}{\partial z}\right)\bigg|_{z=0} = \frac{D_{m,i}}{\delta}\left(C_i\big|_{z=0} - C_i^{TGA}\right) \qquad \left(\frac{\partial C_i}{\partial z}\right)\bigg|_{z=h} = 0$$

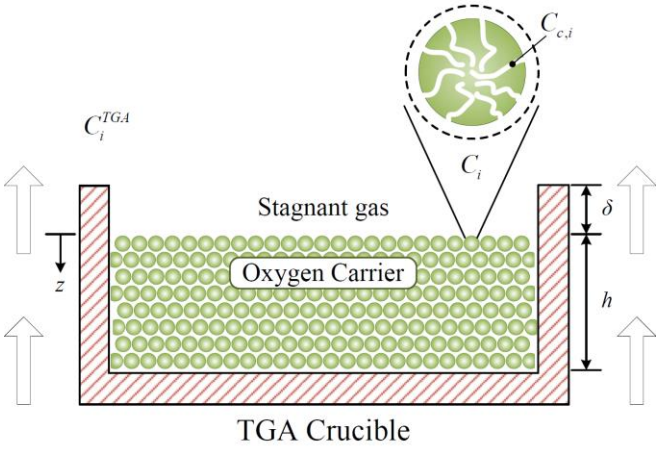

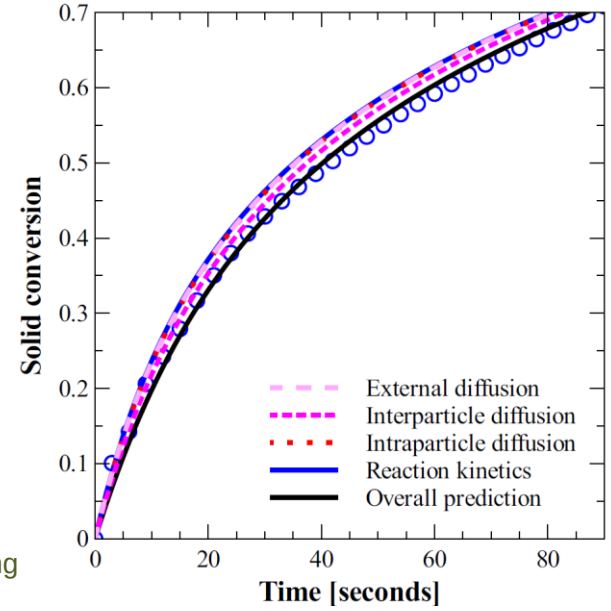

Han, L.; Zhou, Z.; Bollas, G. M. Heterogeneous Modeling of Chemical-Looping Combustion. Part 2: Particle Model. *Chemical Engineering Science* **2013**

Non-catalytic gas-solid reactions

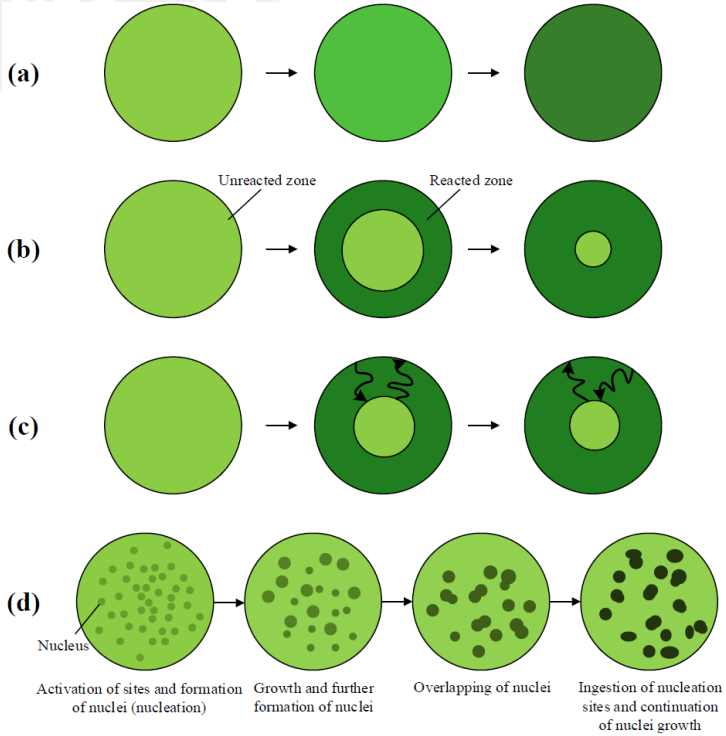

Table 1: Rate and integral expressions for different solid-state kinetic models

No.	Reaction model	$f(x)=1/k\,dx/dt$	$g(x)=kt$	n
F1.5	Three-halves order	$(1-x)^{3/2}$	$2[(1-x)^{(-1/2)}-1]$	0.91
F2	Second-order	$(1-x)^2$	$1/(1-x)-1$	0.83
F3	Third-order	$(1-x)^3$	$(1/2)\left[(1-x)^{-2}-1\right]$	0.70
R1	Zero-order (Polany-Winger equation)	1	x	1.24
R2	Phase-boundary controlled reaction (contracting area, i.e. bi-dimensional shape)	$2(1-x)^{1/2}$	$1-(1-x)^{(1/2)}$	1.11
R3	Phase-boundary controlled reaction (contracting volume, i.e. tridimensional shape)	$3(1-x)^{2/3}$	$1-(1-x)^{(1/3)}$	1.07
D1	One-dimensional diffusion	$1/(2x)$	x^2	0.62
D2	Two-dimensional diffusion Valensi equation	$1/\left[-\ln(1-x)\right]$	$(1-x)\ln(1-x)+x$	0.57
D3	Three-dimensional diffusion Jander equation	$3(1-x)^{(1/3)}/[2(1-x)^{(-1/3)}-1]$	$\left[1-(1-x)^{1/3}\right]^2$	0.54
D4	Three-dimensional diffusion Ginstling – Brounshtein	$3/\left[2(1-x)^{-1/3}-1\right]$	$(1-2x/3)-(1-x)^{(2/3)}$	0.57
AE1	First-order (Mampel) (F1) or Avrami-Erofe'ev (n=1)	$(1-x)$	$-\ln(1-x)$	1
AE0.5	Avrami-Erofe'ev (n=0.5)	$(1/2)(1-x)(-\ln(1-x))^{-1}$	$(-\ln(1-x))^2$	0.50
AE1.5	Avrami-Erofe'ev (n=1.5)	$(3/2)(1-x)\left[-\ln(1-x)\right]^{1/3}$	$(-\ln(1-x))^{2/3}$	1.5
AE2	Avrami-Erofe'ev (n=2)	$2(1-x)\left[-\ln(1-x)\right]^{1/2}$	$(-\ln(1-x))^{1/2}$	2
AE3	Avrami-Erofe'ev (n=3)	$3(1-x)\left[-\ln(1-x)\right]^{2/3}$	$(-\ln(1-x))^{1/3}$	3
AE4	Avrami-Erofe'ev (n=4)	$4(1-x)[-\ln(1-x)]^{(3/4)}$	$(-\ln(1-x))^{1/4}$	4
AEn	Avrami-Erofe'ev	$n(1-x)\left[-\ln(1-x)\right]^{(n-1)/n}$	$(-\ln(1-x))^{1/n}$	n
RPM	Random pore model	$(1-x)(1-\phi\ln(1-x))^{1/2}$	$x=1-\exp\left[-g(x)(1+\phi g(x))\right]$	-
SB	Šesták – Berggren function	$x^m(1-x)^n$		-
PT	Prout-Tompkins	$x(1-x)$	$\ln(x/(1-x))$	-

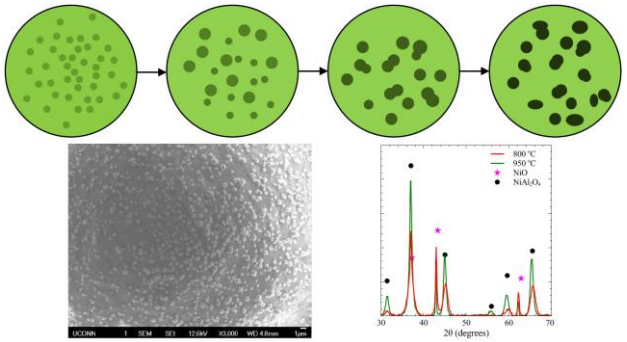

- **Analysis of available literature on reduction of supported and unsupported NiO by H_2**
  - Models of varying degree of fidelity (number of parameters)
  - F-test
  - Akaike Information Criterion

Zhou, Z.; Han, L.; Bollas, G. M. Kinetics of NiO reduction by H_2 and Ni oxidation at conditions relevant to chemical-looping combustion and reforming. Int. Journal of Hydrogen Energy, **2014**

Current experimental setup

- **Fixed-bed apparatus**

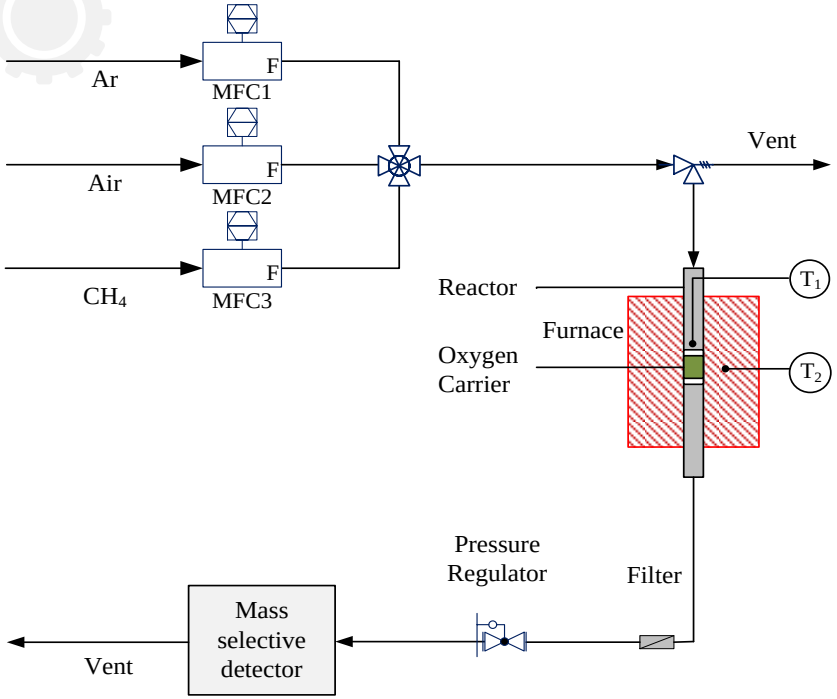

Experimental conditions	
Reduction temperature	800°C
Reduction time	1 min
Reducing gas flow	20 CH_4 + 80 Ar ml/min
Solid loading	2 g
Purge time	3 min
Oxidizing gas	100 air ml/min
Oxidation time	3 min
Tube ID	0.99 cm
Tube length	30 cm

- **NiO/Al_2O_3 oxygen carrier preparation**
  - Dry impregnation with loading of 20 wt% Ni
  - Particle size: 50-150 µm
  - Surface area: 90 m^2/g

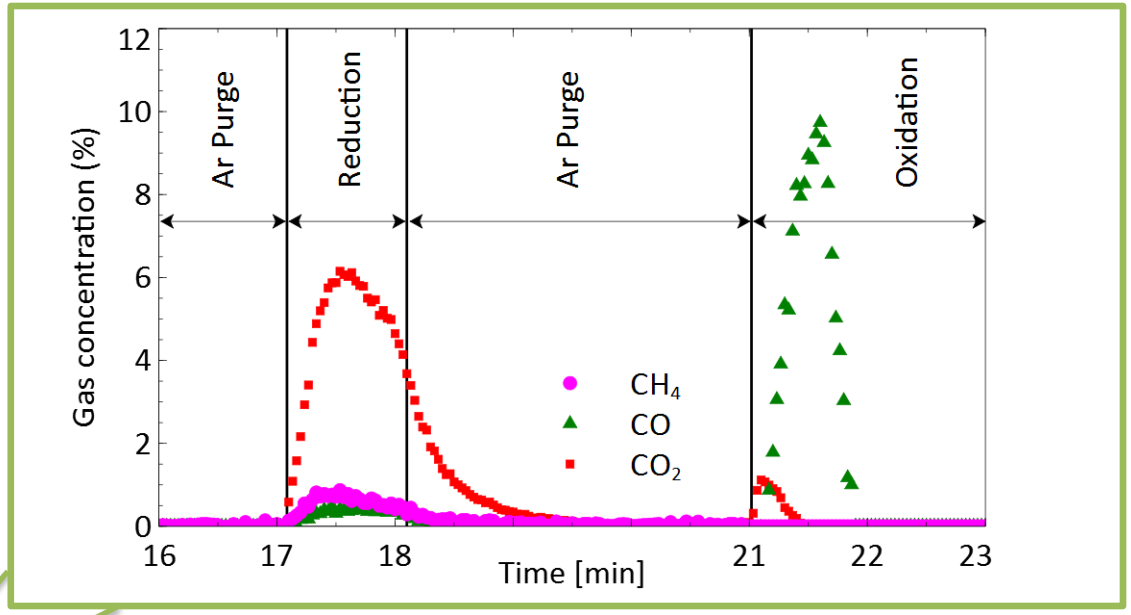
Ar Purge
Reduction
Ar Purge
Oxidation
Gas concentration (%)
Time [min]
CH4
CO
CO2

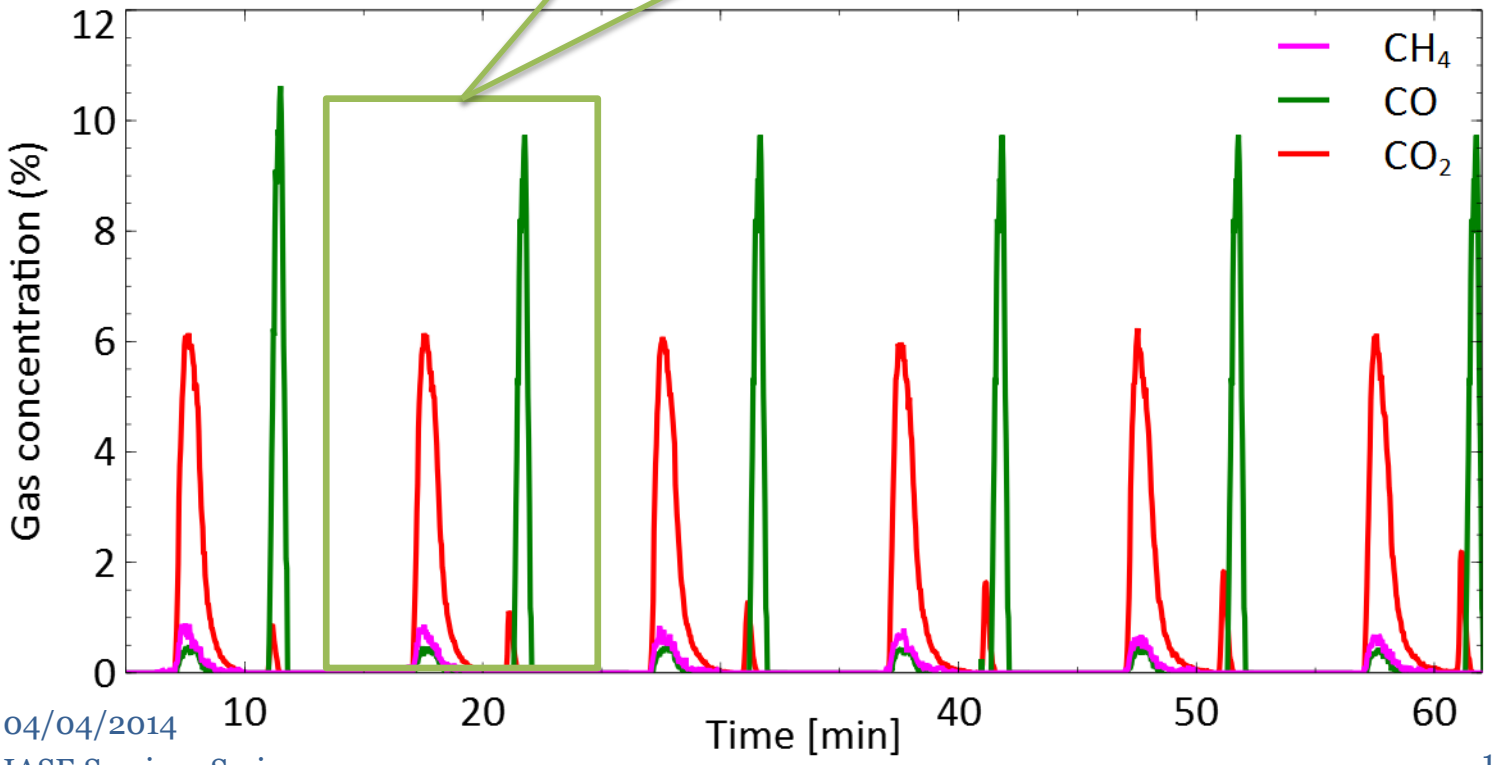
Gas concentration (%)
Time [min]
CH4
CO
CO2

Dynamic Sensitivity Analysis

Model, system of DAE's

$$\mathbf{f}(\dot{\mathbf{x}}(t), \mathbf{x}(t), \mathbf{u}(t), \bar{\mathbf{w}}, \boldsymbol{\theta}, t) = 0$$
$$\hat{\mathbf{y}}(t) = \mathbf{h}(\mathbf{x}(t))$$

$\mathbf{f}$: continuous function
$\dot{\mathbf{x}}(t)$: differential state variables
$\mathbf{u}(t)$: time-varying controls
$\bar{\mathbf{w}}$: time-constant controls
$\boldsymbol{\theta}$: parameter vector
$\mathbf{h}(\mathbf{x}(t))$: measured state variables
$\hat{\mathbf{y}}(\mathrm{t})$: measured responses

Sensitivity matrix

$$Q = \begin{bmatrix} \frac{\partial \hat{y}_1}{\partial \theta_i} & \cdots & \frac{\partial \hat{y}_1}{\partial \theta_p} \\ \vdots & \ddots & \vdots \\ \frac{\partial \hat{y}_n}{\partial \theta_i} & \cdots & \frac{\partial \hat{y}_n}{\partial \theta_p} \end{bmatrix}$$

Local methods

Differentiation of model equations

$$\frac{\mathrm{d}}{\mathrm{dt}}\frac{\partial \hat{\mathbf{y}}}{\partial \boldsymbol{\theta}} = \frac{\partial \mathbf{f}}{\partial \hat{\mathbf{y}}} \cdot \frac{\partial \hat{\mathbf{y}}}{\partial \theta} + \frac{\partial \mathbf{f}}{\partial \boldsymbol{\theta}}$$

Results for CLC fixed-bed reactor:

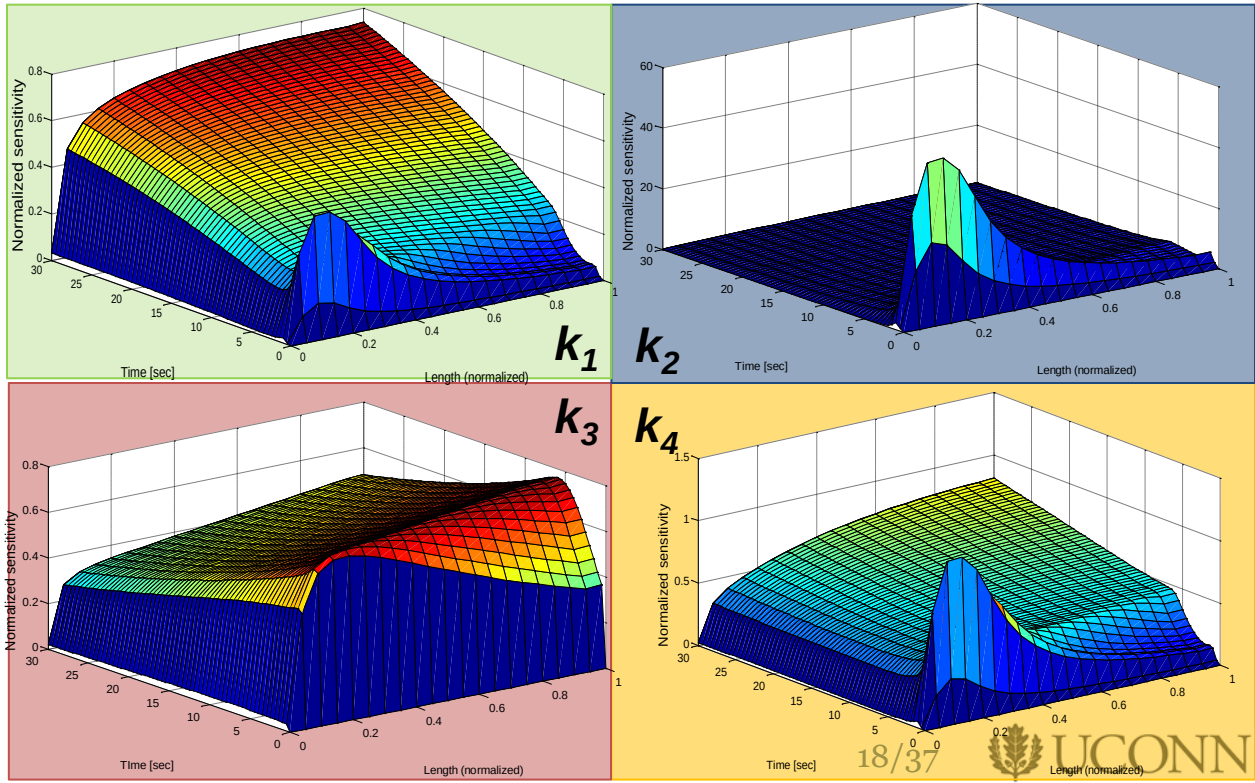

Identifiability Analysis

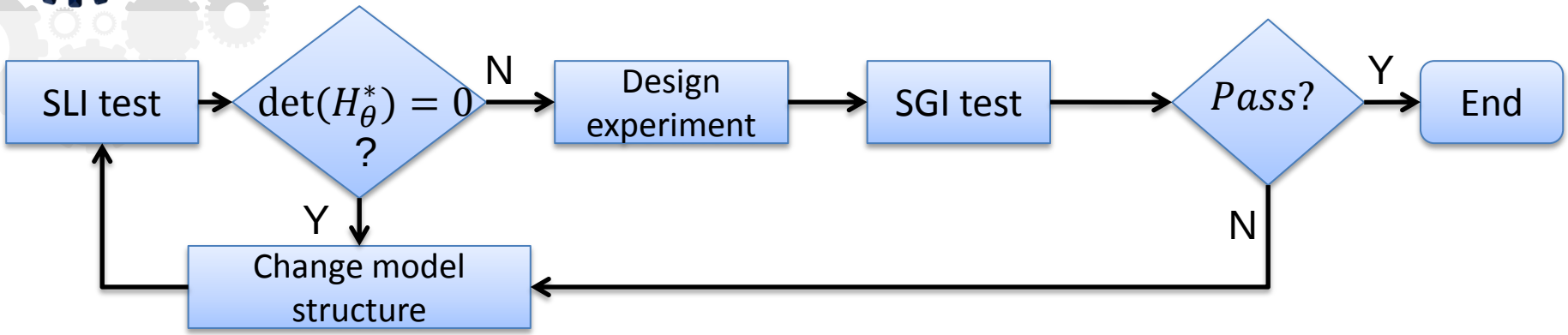

- **Structural local identifiability test (SLI)**
  - (1) Correlation of sensitivity matrix is different from ± 1
  - (2) Fisher information matrix is non-singular

$$\mathbf{H}_\theta^* = \sum_{i=1}^{N_{ts}} \sum_{j=1}^{N_y} \sigma_{ij} \mathbf{Q}_i^T \mathbf{Q}_j$$

- **Structural global identifiability test (SGI)**
  - Verifies if parameter sets do not provide the same model responses

$$\Phi^I = \max_{\boldsymbol{\theta},\boldsymbol{\theta}^*} \left(\boldsymbol{\theta} - \boldsymbol{\theta}^*\right)^T \mathbf{W}_\theta \left(\boldsymbol{\theta} - \boldsymbol{\theta}^*\right) \le \varepsilon_\theta$$

Subject to:

$$\int_0^\tau \left(\mathbf{y}(\mathbf{u}_0, \boldsymbol{\theta}) - \mathbf{y}(\mathbf{u}_0, \boldsymbol{\theta}^*)\right)^T \mathbf{W}_y \left(\mathbf{y}(\mathbf{u}_0, \boldsymbol{\theta}) - \mathbf{y}(\mathbf{u}_0, \boldsymbol{\theta}^*)\right) dt < \varepsilon_y$$

$\boldsymbol{\theta}, \boldsymbol{\theta}^*$: parameter sets
$\mathbf{y}$: model trajectory
$\boldsymbol{u_0}$: initial controls
$\mathbf{W}$: weights
$\varepsilon_\theta, \varepsilon_y$: small numbers

Identifiability Analysis: Arrhenius Expression

- **Arrhenius Expression:**

$$k = k_{ref} \exp\left[-\frac{E}{R}\left(\frac{1}{T} - \frac{1}{T_{ref}}\right)\right]$$

- **SLI results:**
  - 1 experiment
    - *High correlation*
    - *Unidentifiable*
  - 2 experiments
    - *Identifiable*

Optimal experiments		
T [°C]	600	800
Q_{CH4} [sccm]	30	30
Solids [g]	1.2	2.2

- **SGI results:**
  - $\Phi^I = 4\text{E-}10 < \varepsilon_\theta = 1\text{E-}6$
  - $\varepsilon_y = 1\text{E-}3$

Correlation matrix of Arrhenius parameters

	Ea_1	Ea_2	Ea_3	Ea_4	k_1	k_2	k_3	k_4
Ea_1	1.000							
Ea_2	-0.394	1.000						
Ea_3	-0.247	-0.022	1.000					
Ea_4	-0.140	-0.143	-0.589	1.000				
k_1	-0.817	0.287	0.644	-0.271	1.000			
k_2	-0.396	1.000	-0.025	-0.140	0.289	1.000		
k_3	-0.290	-0.017	0.999	-0.575	0.666	-0.019	1.000	
k_4	-0.052	0.316	-0.165	-0.573	0.045	0.317	-0.158	1.000

Correlation matrix of Arrhenius parameters

	Ea_1	Ea_2	Ea_3	Ea_4	k_1	k_2	k_3	k_4
Ea_1	1.000							
Ea_2	-0.108	1.000						
Ea_3	-0.917	0.199	1.000					
Ea_4	-0.726	0.164	0.810	1.000				
k_1	-0.385	0.035	0.213	-0.002	1.000			
k_2	-0.134	-0.044	0.317	0.339	-0.048	1.000		
k_3	-0.758	0.193	0.886	0.818	-0.214	0.333	1.000	
k_4	0.027	0.166	0.047	-0.050	-0.291	-0.053	0.145	1.000

Han L, Zhou Z, Bollas GM. Optimal Experimental Design for Fixed Bed Chemical-Looping Experiments. Comput Chem Eng 2014

Model-guided experiment

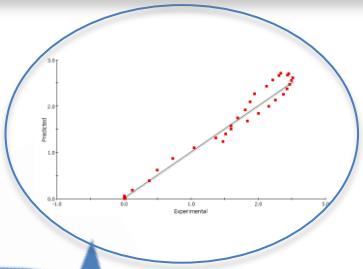

Estimate parameters & confidence intervals

Build first principles process model

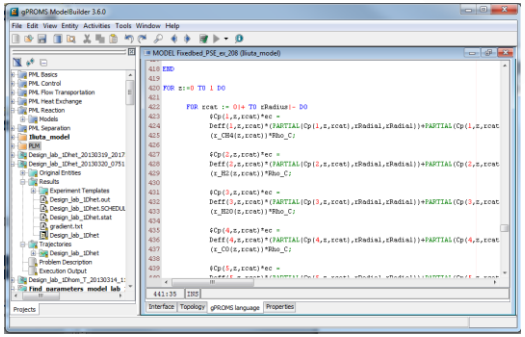

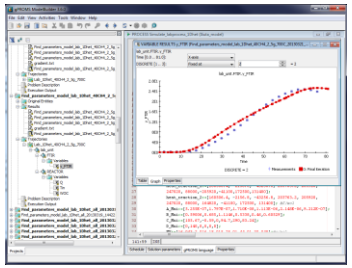

Design optimal experiment

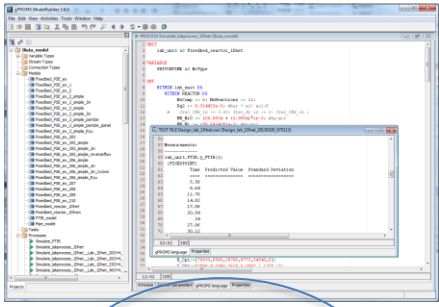

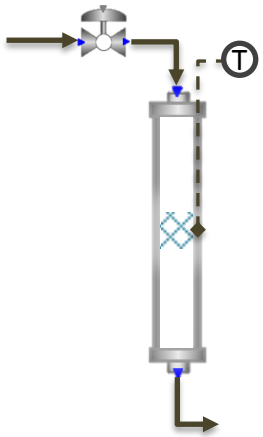

Conduct experiment at specified conditions

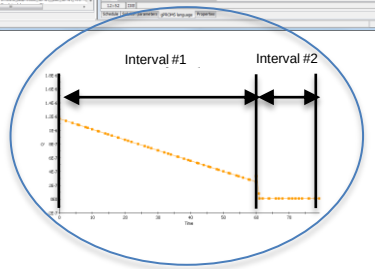

Optimal experimental design (OED)

- **Motivation:** maximize information content for parameter estimation

$$\boldsymbol{\varphi}^{opt} = \arg\min_{\boldsymbol{\varphi}} \left[\det \left(\boldsymbol{H}_{\boldsymbol{\theta}}^{-1}(\boldsymbol{\theta}, \boldsymbol{\varphi}) \right) \right]$$

subject to:

$$\mathbf{f}(\dot{\mathbf{x}}(t), \mathbf{x}(t), \mathbf{u}(t), \bar{\mathbf{w}}, \boldsymbol{\theta}, t) = 0$$

$$\varphi_i^L \leq \varphi_i \leq \varphi_i^U$$

Design criterion:
D-OPTIMALITY

- **Model + experimental results**

Experiments		
	Standard	Optimal
T [°C]	700	700
Q_{CH4} [sccm]	10	20
Solids [g]	2	2

Comparison of optimal (-) and baseline (--) experiments

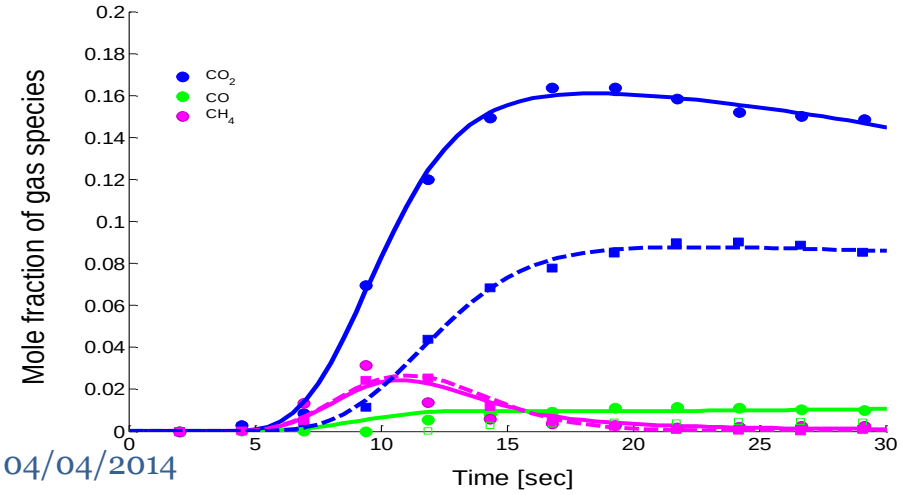

Norm 95% confidence interval

Kinetics	Nominal exp.	Optimal exp.
k_1	0.3880	0.1654
k_2	1.4416	0.8379
k_3	0.6005	0.1461
k_4	3.2706	0.3118

Improves parameter estimation for all uncertain kinetic parameters

Fluidized bed model

Kunii & Levenspiel 3-phase model

Mass balance

- **Gas (bubble)**

$$(\delta+\alpha\delta\varepsilon_{mf})\frac{\partial C_{j,b}}{\partial t}+\frac{\partial(u_b(\delta+\alpha\delta\varepsilon_{mf})C_{j,b})}{\partial z}=K_{j,be}(C_{j,e}-C_{j,b})(\delta+\alpha\delta\varepsilon_{mf})+(\lambda_1 C_{j,b}+\lambda_2 C_{j,e})\frac{\partial(u_b(\delta+\alpha\delta\varepsilon_{mf}))}{\partial z}+R_{j,b}(C_{j,b})\rho_P\alpha\delta(1-\varepsilon_{mf})$$

- **Gas (emulsion)**

$$(1-\delta-\alpha\delta)\varepsilon_{mf}\frac{\partial C_{j,e}}{\partial t}+\frac{\partial(u_e(1-\delta-\alpha\delta)\varepsilon_{mf}C_{j,e})}{\partial z}=K_{j,eb}(C_{j,b}-C_{j,e})(1-\delta-\alpha\delta)\varepsilon_{mf}-(\lambda_1 C_{j,b}+\lambda_2 C_{j,e})\frac{\partial(u_b(\delta+\alpha\delta\varepsilon_{mf}))}{\partial z}+R_{j,e}(C_{j,e})\rho_P(1-\delta-\alpha\delta)(1-\varepsilon_{mf})$$

- **Solid (wake)**

$$\alpha\delta(1-\varepsilon_{mf})\rho_P\frac{\partial C_{i,w}}{\partial t}+\frac{\partial(u_b\alpha\delta(1-\varepsilon_{mf})\rho_P C_{i,w})}{\partial z}=K_{j,we}(C_{i,e}-C_{i,w})\rho_P\alpha\delta(1-\varepsilon_{mf})+(\lambda_1 C_{i,w}+\lambda_2 C_{i,e})\frac{\partial(u_b\alpha\delta(1-\varepsilon_{mf})\rho_P)}{\partial z}+R_{i,w}M_i\rho_P\alpha\delta(1-\varepsilon_{mf})$$

- **Solid (emulsion)**

$$(1-\delta-\alpha\delta)(1-\varepsilon_{mf})\rho_P\frac{\partial C_{ie}}{\partial t}+\frac{\partial(u_s(1-\delta-\alpha\delta)(1-\varepsilon_{mf})\rho_P C_{i,e})}{\partial z}=K_{j,ew}(C_{i,w}-C_{i,e})(1-\delta-\alpha\delta)(1-\varepsilon_{mf})-(\lambda_1 C_{i,w}+\lambda_2 C_{i,e})\frac{\partial(u_b\alpha\delta(1-\varepsilon_{mf})\rho_P)}{\partial z}+R_{i,w}M_i\rho_P(1-\delta-\alpha\delta)(1-\varepsilon_{mf})$$

- **Gas (freeboard)**

$$\varepsilon_f\frac{\partial C_{j,f}}{\partial t}+u_{g,f}\frac{\partial C_{j,f}}{\partial z}=(1-\varepsilon_f)R_{j,f}\rho_p$$

- **Solid (freeboard)**

$$(1-\varepsilon_f)\frac{\partial C_{i,f}}{\partial t}+u_{s,f}\frac{\partial C_{i,f}}{\partial z}=(1-\varepsilon_f)R_{i,f}M_i$$

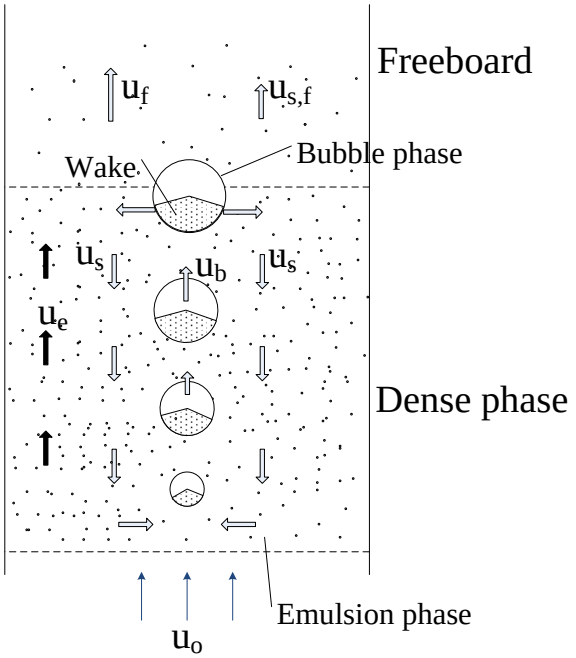

Energy balance

- **Bubble**

$$\left((\delta+\alpha\delta\varepsilon_{mf})Cp_b C_{g,b}+\alpha\delta(1-\varepsilon_{mf})\rho_P\sum Cp_{w,s,i}\,C_{w,s,i}/M_i\right)\frac{\partial T_b}{\partial t}+\left((\delta+\alpha\delta\varepsilon_{mf})C_{g,b}Cp_b u_b+\alpha\delta(1-\varepsilon_{mf})u_b\rho_P\sum Cp_{e,s,i}\,C_{e,s,i}/M_i\right)\frac{\partial T_b}{\partial z}=(\delta+\alpha\delta\varepsilon_{mf})H_{be}(T_e-T_b)+\alpha\delta(1-\varepsilon_{mf})\sum(-\Delta H_{i,b})(-R_{i,b})\rho_P+(\lambda_1 T_b Cp_b C_{g,b}+\lambda_2 T_e Cp_e C_{g,e}+\sum(\lambda_1 T_b Cp_{w,s,i}\,C_{w,s,i}/M_i+\lambda_2 T_e Cp_{e,s,i}C_{e,s,i}/M_i))\frac{\partial}{\partial z}(u_b(\delta+\alpha\delta\varepsilon_{mf}))$$

- **Emulsion**

$$\left((1-\delta-\alpha\delta)\varepsilon_{mf}Cp_e C_{g,e}+\rho_P(1-\delta-\alpha\delta)(1-\varepsilon_{mf})\sum C_{e,s,i}Cp_{e,s,i}/M_i\right)\frac{\partial T_e}{\partial t}+\left((1-\delta-\alpha\delta)\varepsilon_{mf}C_{g,e}Cp_e u_e+\rho_P(1-\delta-\alpha\delta)(1-\varepsilon_{mf})u_s\sum C_{e,s,i}Cp_{e,s,i}/M_i\right)\frac{\partial T_e}{\partial z}=(1-\delta-\alpha\delta)\varepsilon_{mf}H_{eb}(T_b-T_e)+(1-\delta-\alpha\delta)(1-\varepsilon_{mf})\sum(-\Delta H_{i,e})(-R_{i,e})\rho_P-\left(\lambda_1 T_b Cp_b C_{g,b}+\lambda_2 T_e Cp_e C_{g,e}+\sum\left(\lambda_1 T_b Cp_{w,s,i}\frac{C_{w,s,i}}{M_i}+\frac{\lambda_2 T_e Cp_{e,s,i}C_{e,s,i}}{M_i}\right)\right)\frac{\partial}{\partial z}(u_b(\delta+\alpha\delta\varepsilon_{mf}))+U(T_a-T_e)/H_d$$

- **Freeboard**

$$\varepsilon_f Cp_f C_{g,f}\frac{\partial T_f}{\partial t}+Cp_f C_{g,f}u_f\frac{\partial T_f}{\partial z}=\sum(-\Delta H_{i,f})(-R_{i,f})\rho_P+U(T_a-T_f)/H_f$$

Zhou, Z.; Han, L.; Bollas, G. M. Modeling Chemical-Looping Combustion in Bubbling Fluidized Bed Reactors. *AIChE J.* **2014**

Fluidized bed operation

- ***Fluidized Bed chemical-looping – prediction and analysis***

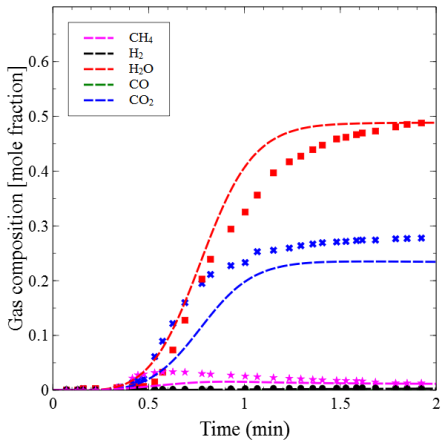

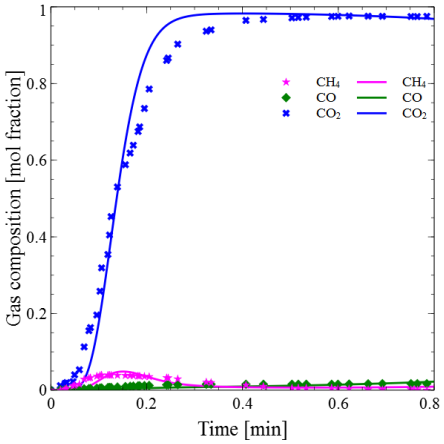

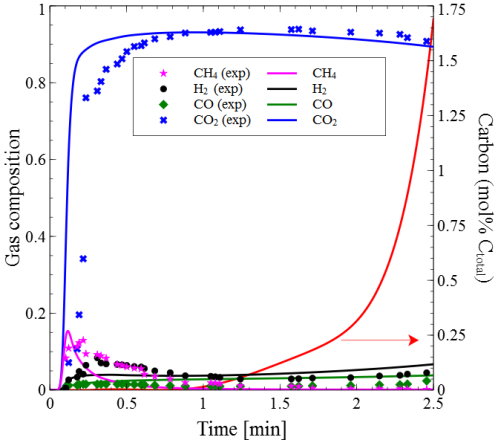

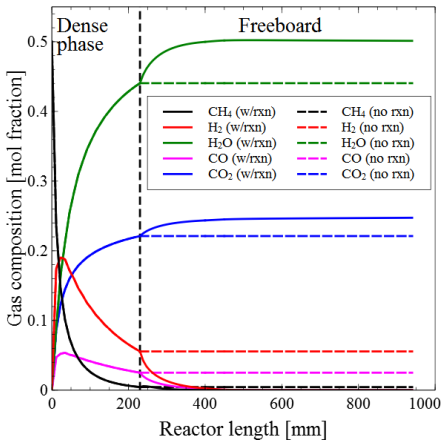

- *Model is predictive (kinetic mechanism and constants of the fixed bed models used)*
- *Freeboard contributes significantly to CH_4 conversion and completion of oxidation*
- *Consistent with all relevant experimental observations from various laboratories*

- Zhou, Z.; Han, L.; Bollas, G. M. Modeling Chemical-Looping Combustion in Bubbling Fluidized Bed Reactors. *AIChE J.* **2014**
- Zhou, Z.; Han, L.; Bollas, G. M. Overview of chemical-looping reduction in fixed-bed and fluidized-bed reactors focused on oxygen carrier utilization and reactor efficiency. *Aerosol & Air Quality Research.* **2014**

Fixed/Fluidized beds comparison

- **Comprehensive comparison of two reactor designs (fixed and fluidized bed) of the same oxygen carrier loading**
- **The fixed bed reactor is inferior in all aspects including**
  - CO_2 selectivity
  - Carbon formation
  - Bed isothermality

Zhou Z, Han L, Bollas GM, Overview of Chemical-Looping Reduction in Fixed Bed and Fluidized Bed Reactors Focused on Oxygen Carrier Utilization and Reactor Efficiency. Aerosol Air Qual Res **2014**;14:559–71

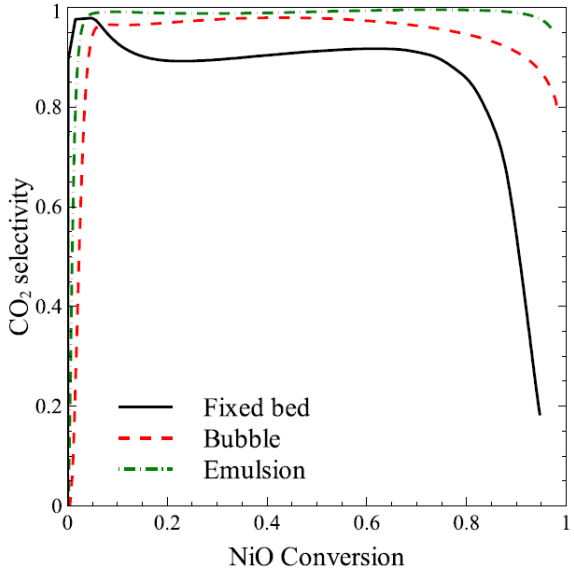

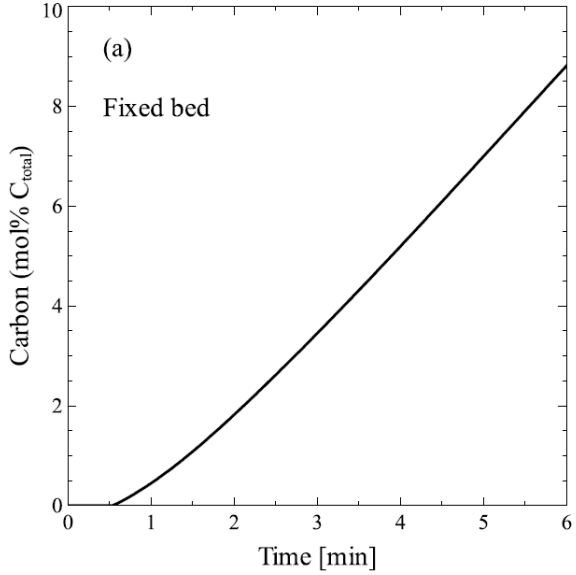

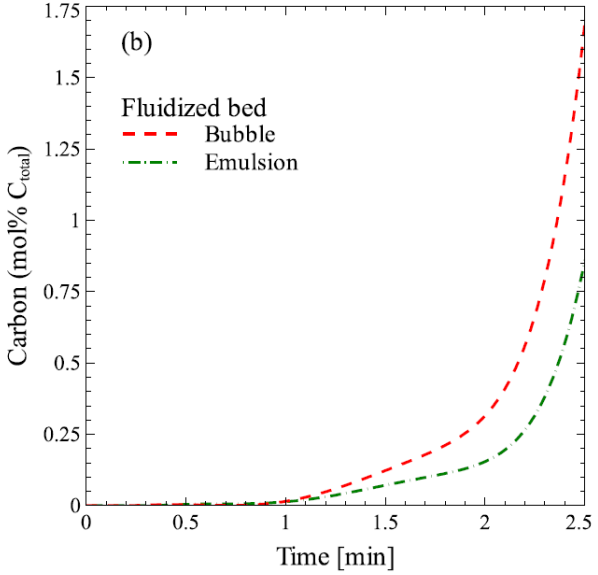

Summary of background

- **Chemical-Looping**
  - Most efficient method for CO_2 capture
  - Very high research effort
  - Tremendous research expenditure
  - Combustion or reforming are feasible
  - Mature process
- **Process Options**
  - Fluidized beds
  - Fixed beds
  - Rotary beds
  - Rotating beds
  - Moving beds
- **Our work**
  - Modeled <u>all</u> fixed bed reactors with CH_4 and NiO
  - Predicted <u>all</u> fluidized beds with CH_4 & NiO
  - Compared fixed and fluidized bed CLC and CLR
  - Setup a bench-scale fixed bed reactor

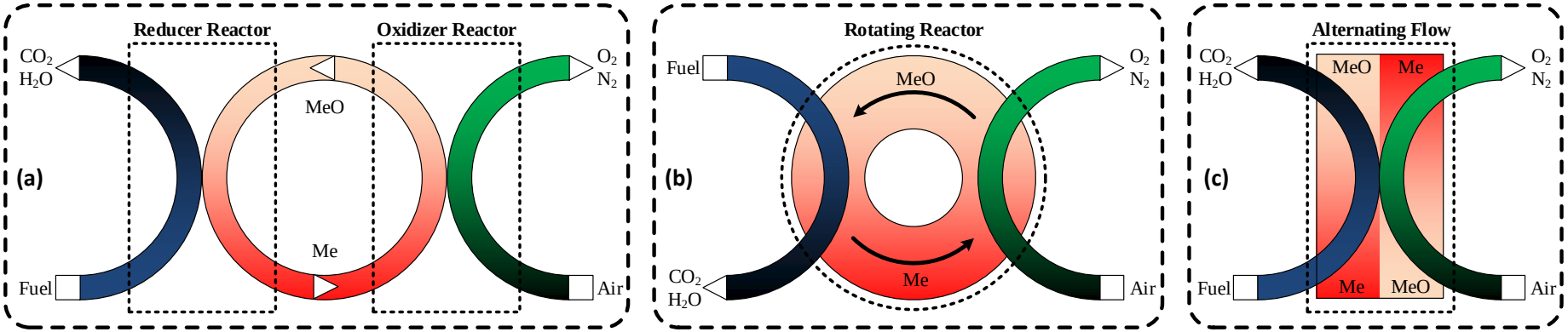

Reactor options for Chemical-looping Combustion (CLC): (a) circulating fluidized-bed; (b) rotating reactor; and (c) alternating flow over a fixed-bed.

Typical fixed-bed experiment

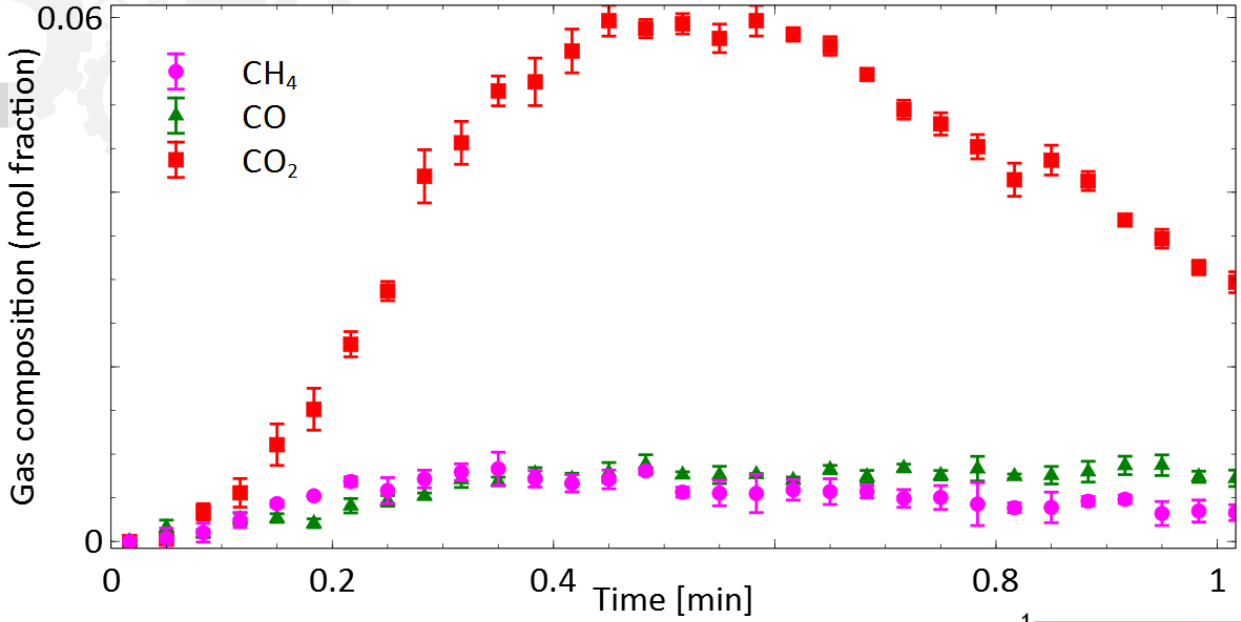

Experimental settings	
Reduction temperature	800°C
Reduction time	1 min
Reducing gas flow	10 CH_4 in 100 ml/min
Solid loading	2 g

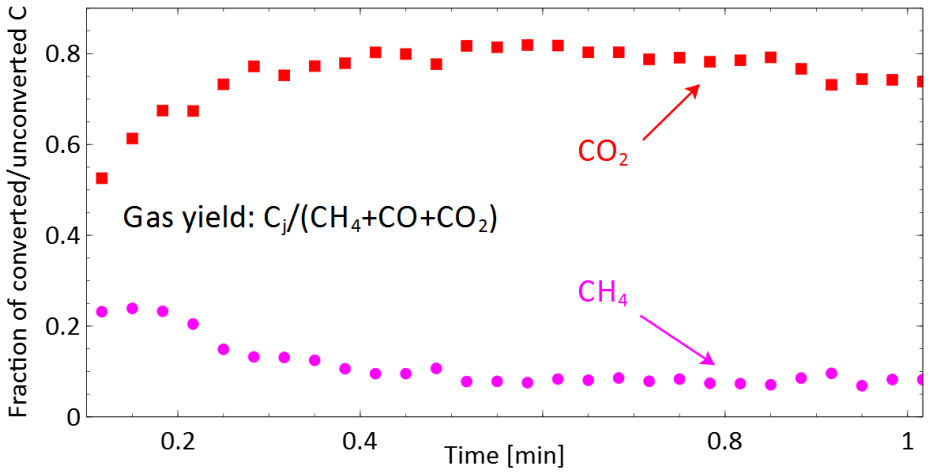

Oxygen carrier conversion

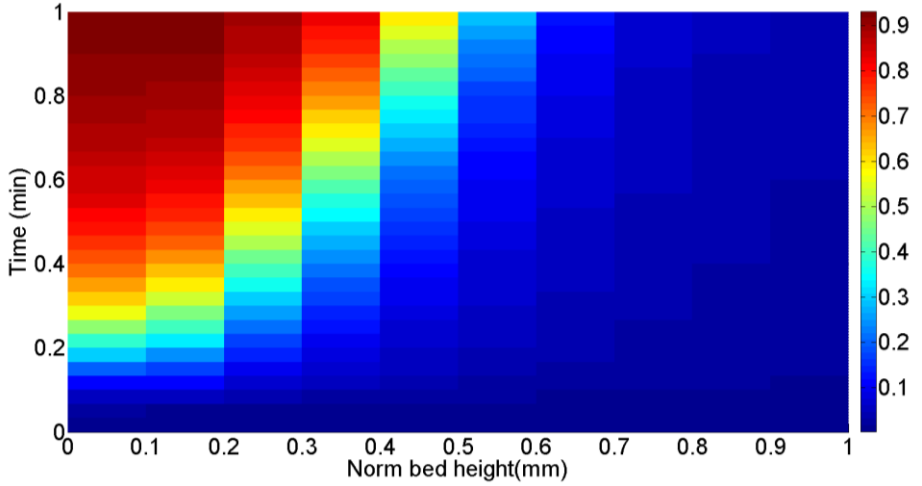

Reverse-Flow Fixed-bed CLC Reactor

- Design of the novel reactor setup

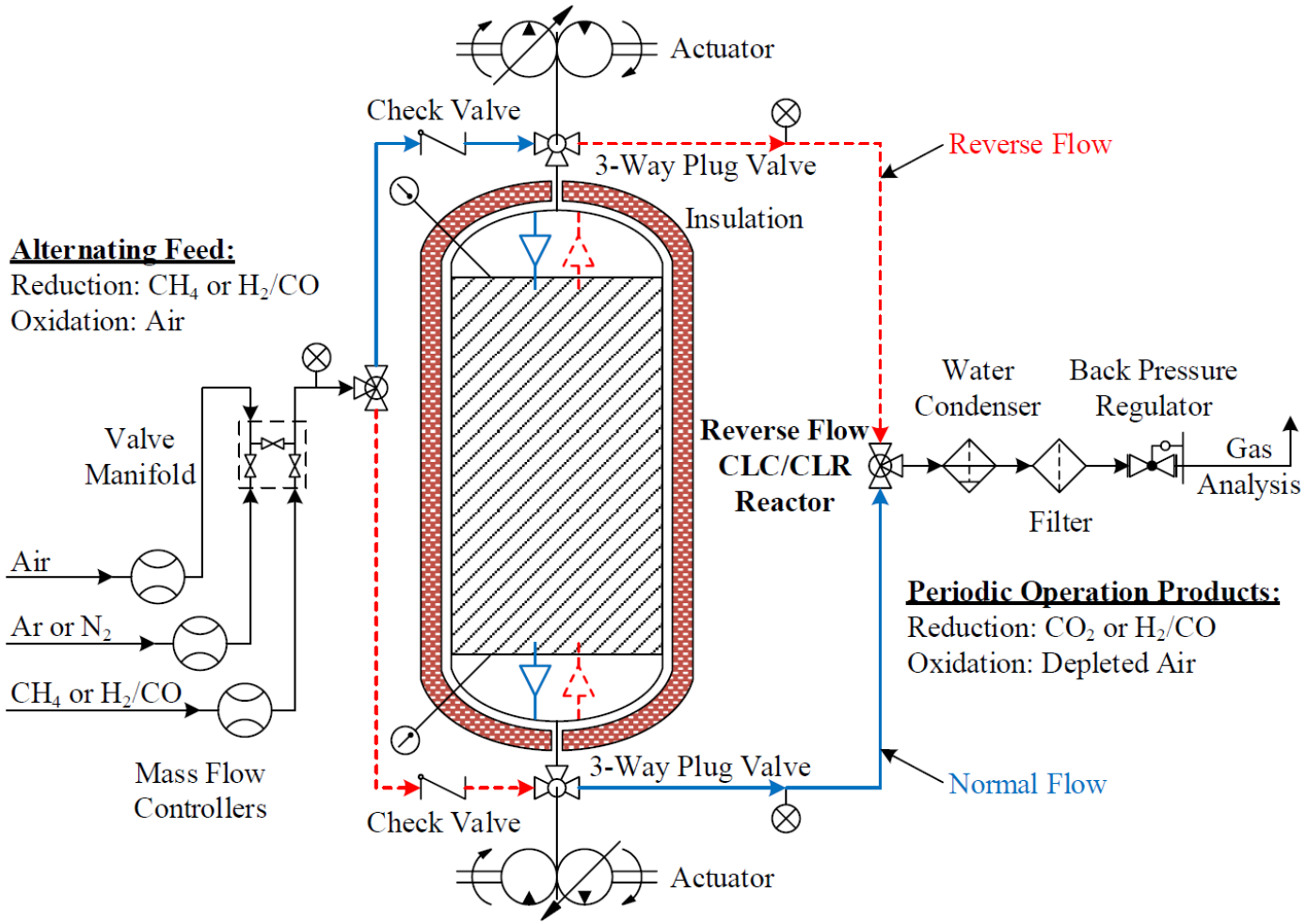

Patent Claims (Bollas, Han 2014)

- ***A novel fixed-bed chemical-looping reactor configuration was invented, in which the fuel flow direction is periodically switched during each cycle*.**
- **The new design significantly improves the performance of fixed-bed chemical-looping reactors, making them competitive to their fluidized-bed equivalents, while overcoming their operating bottlenecks.**
- **The novel system enables:**
  - *(1) improved oxygen carrier utilization,*
  - *(2) higher CO_2 capture efficiency (by up to 50%),*
  - *(3) mitigation of hot and cold zones,*
  - *(4) elimination of gas-solids separation steps,*
  - *(5) resistance to carbon deposition*.
- **Advantages relevant to the oxygen carrier used (as compared to current process configurations) relate to the elimination of:**
  - *(6) need for oxygen carrier fluidizability,*
  - *(7) attrition,*
  - *(8) toxic solid fines effluents,*
  - *(9) need for oxygen carrier addition*.

Reverse-Flow Fixed-bed Reactor Model

Model Description

- 1D heterogeneous model
- Dusty-gas model (concentrated transport)
- Time varying boundary conditions for the fluid phase

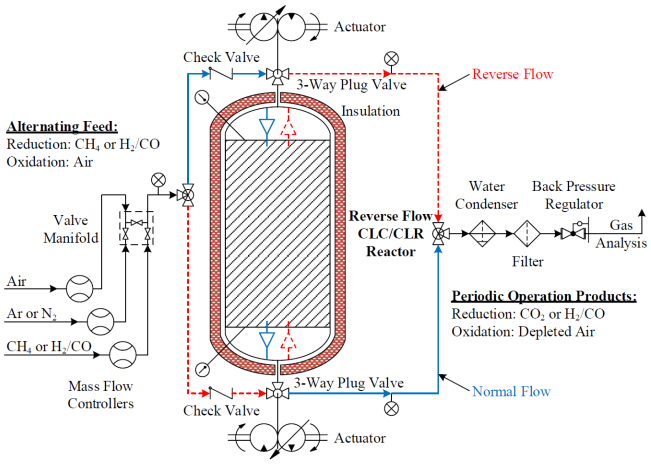

Full heterogeneous design equations

Solid phase

$$-\frac{\partial C_{c,i}}{\partial r_c}=\sum_{j=1}^{N}\frac{1}{D_{ij}^{e}}\left(y_k J_i-y_i J_k\right)+\frac{J_i}{D_{iK}^{e}}$$

$$\frac{\partial(\varepsilon_c C_{c,i})}{\partial t}+\frac{1}{r_c^{\,2}}\frac{\partial}{\partial r_c}\left(r_c^{\,2}J_i\right)=\rho_s\sum R_i$$

$$\left((1-\varepsilon_c)\rho_s C_{p,s}+\varepsilon_c C_{p,c}C_{T,c}\right)\frac{\partial T_c}{\partial t}=\frac{1}{r_c^{\,2}}\frac{\partial}{\partial r}\left(r_c^{\,2}\lambda_s\frac{\partial T_c}{\partial r_c}\right)+\rho_s\sum\left(-\Delta H_i\right)(R_i)$$

$$J_i\big|_{r_c=0}=\left.\frac{\partial T_c}{\partial r_c}\right|_{r_c=0}=0 \qquad J_i\big|_{r_c=r_p}=k_{c,i}\left(C_{c,i}\big|_{r_c=r_p}-C_i\right)$$

$$-\lambda_s\left(\frac{\partial T_c}{\partial r_c}\right)\Big|_{r_c=r_p}=h_f\left(T_c\big|_{r_c=r_p}-T\right)$$

Fluid phase

$$\frac{\partial(\varepsilon_b C_i)}{\partial t}+\frac{\partial(uC_i)}{\partial z}=\varepsilon_b\frac{\partial}{\partial z}\left(D_{ax,i}\frac{\partial C_i}{\partial z}\right)+k_{c,i}a_v\left(C_{c,i}\big|_{r_c=r_p}-C_i\right)$$

$$\frac{\partial(\varepsilon_b C_{p,f}C_T T)}{\partial t}+\frac{\partial(\mathrm{C}_T\,C_{p,f}uT)}{\partial z}=\varepsilon_b\frac{\partial}{\partial z}\left(\lambda_{ax}\frac{\partial T}{\partial z}\right)+h_f a_v\left(T_c\big|_{r_c=r_p}-T\right)$$

$$\frac{dP}{dz}=-\left(\frac{1-\varepsilon_b}{\varepsilon_b^{\,3}}\right)\left(\frac{\rho u_0^2}{d_p}\right)\left(\frac{150}{Re_p}+1.75\right)$$

$$U(t)=\kappa(t)u$$

$$\kappa(t)=\begin{cases}1, & t\in\left[(n-1)t_s,(n-1/2)t_s\right]\\ -1, & t\in\left[(n-1/2)t_s,nt_s\right]\end{cases}$$

$$\varepsilon_b D_{ax,i}\frac{\partial C_i}{\partial z}=\begin{cases}\dfrac{1+\kappa(t)}{2}u\left(C_i-C_{i,\mathrm{in}}\right), & z=0\\ -\dfrac{1-\kappa(t)}{2}u\left(C_i-C_{i,\mathrm{in}}\right), & z=L\end{cases}$$

$$\varepsilon_b\lambda_{ax}\frac{\partial T}{\partial z}=\begin{cases}\dfrac{1+\kappa(t)}{2}u\left(T-T_{in}\right)C_T C_{p,f}, & z=0\\ -\dfrac{1-\kappa(t)}{2}u\left(T-T_{in}\right)C_T C_{p,f}, & z=L\end{cases}$$

$$P\big|_{z=L}=P_{out}$$

Han L, Zhou Z, Bollas GM. Chemical-looping combustion in a reverse-flow fixed-bed reactor. Applied Energy 2014

Performance metrics I

- **CH_4 conversion and CO_2 selectivity**

Table: *CO_2 capture efficiency for varying oxygen carrier conversion*

Solid conversion	One-directional	Reverse-flow
0.3	0.9238	0.9559
0.4	0.8975	0.9513
0.5	0.8692	0.9347
0.6	0.8389	0.9105
0.7	0.8055	0.8854
0.8	0.7652	0.8508

← Bench-scale reactor

Solid conversion	One-directional	Reverse-flow
0.3	0.9102	0.9387
0.4	0.8759	0.9239
0.5	0.8399	0.9012
0.6	0.8020	0.8810
0.7	0.7619	0.8525
0.8	0.7146	0.8144

Industrial-scale reactor →

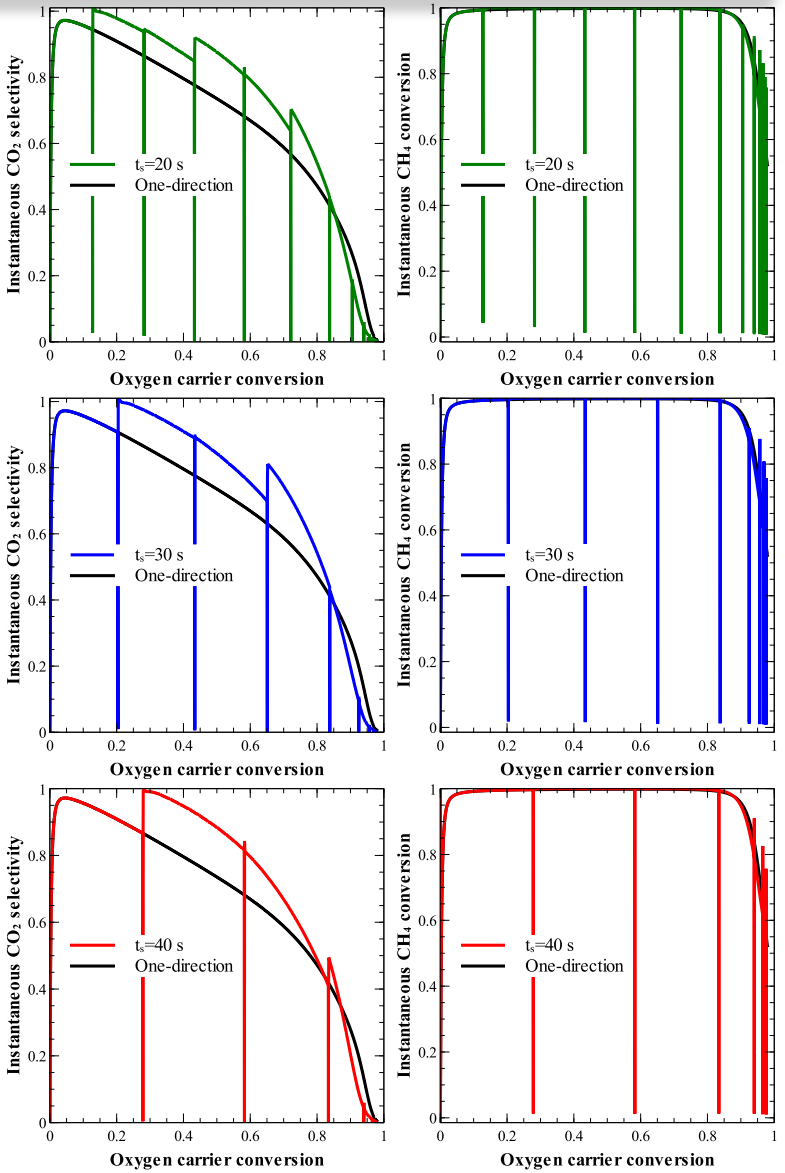

- Reactor in this study is suboptimal for fair comparison with existing fixed bed reactors

Han L, Zhou Z, Bollas GM. Chemical-looping combustion in a reverse-flow fixed-bed reactor. Applied Energy 2014

Bollas GM, Han L. Reverse-Flow Reactor for Chemical-Looping Combustion and Reforming of Gaseous Fuels; US Provisional Patent - University of Connecticut, 2014.

Performance metrics II

Oxygen carrier conversion

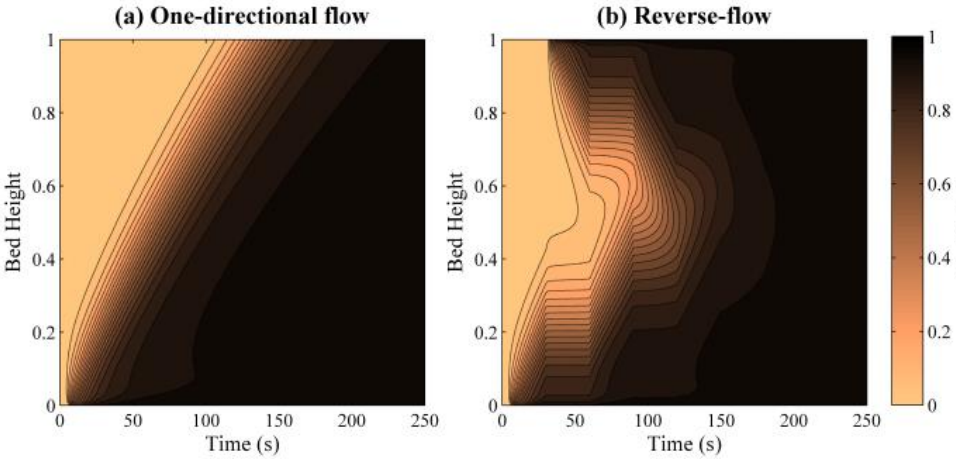

Bed Temperature Profile

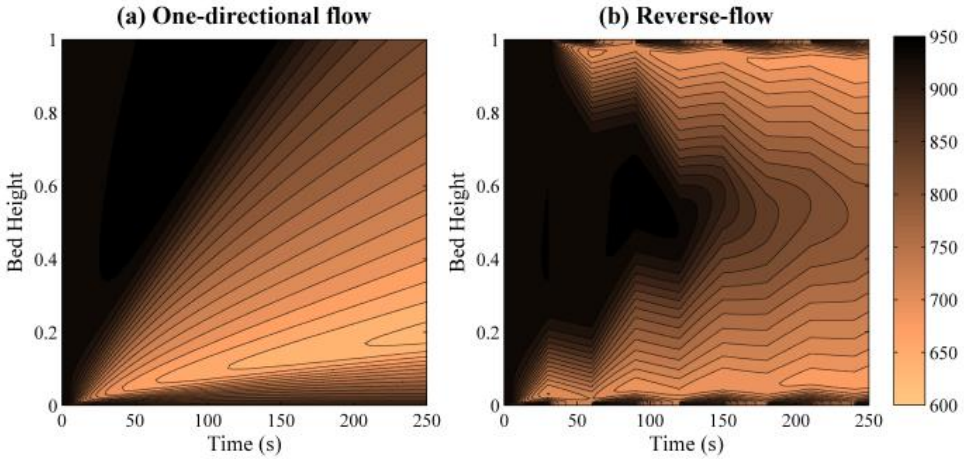

Carbon Formation

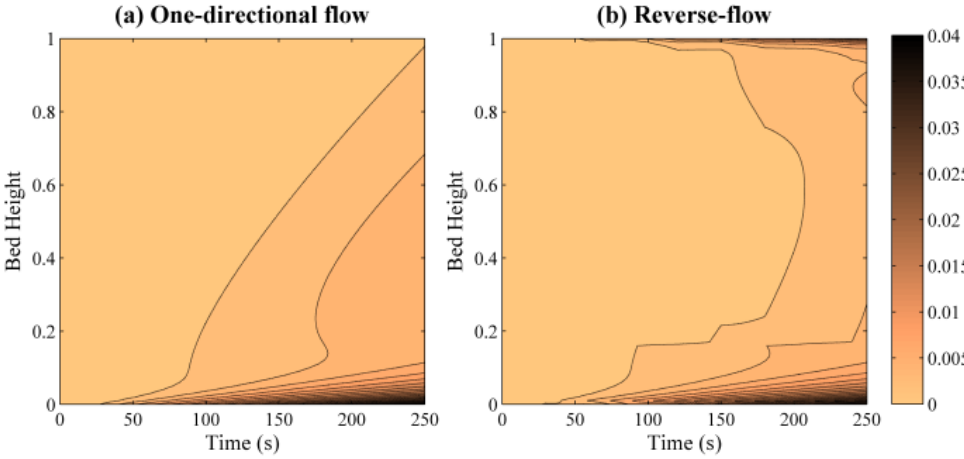

Solid Carbon selectivity and Max Bed T drop

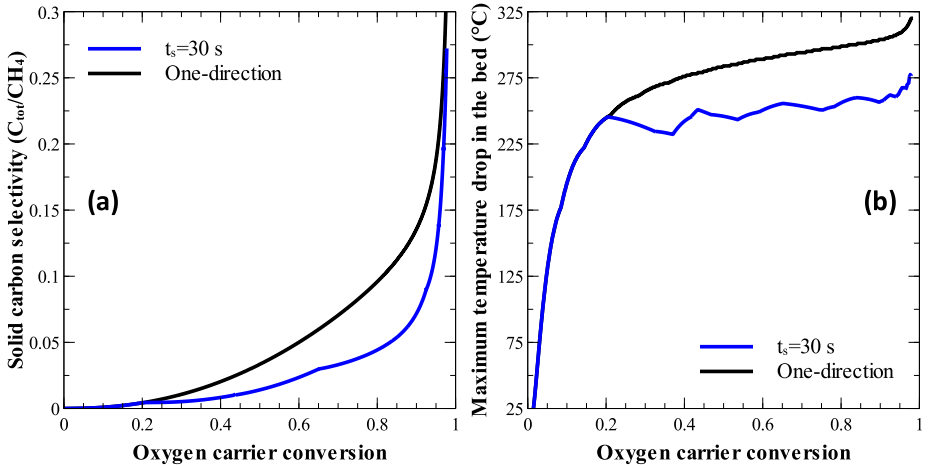

Han L, Zhou Z, Bollas GM. Chemical-looping combustion in a reverse-flow fixed-bed reactor. Applied Energy 2014

Scaled-up Performance metrics I

- **Scale-up procedure**
  - Commercially realistic industrial-scale fixed-bed reactor
  - Small particle size (300 µm) to minimize diffusion effects
  - Significant pressure drop in the system =>
    - *Constraint: bed height should not exceed 1 m*
  - Scaling factors:
    - *L/D ratio and Froude number*

	Bench-scale reactor	Industrial-scale reactor
L [m]	0.22	1.0
D [m]	0.055	0.25
Q (L/min)	16.68 (100% CH_4)	3000 (100% CH_4)
Fr	0.34	0.39
L/D	4	4
Re_p	0.80	6.9
ΔP [bar]	0.3	4

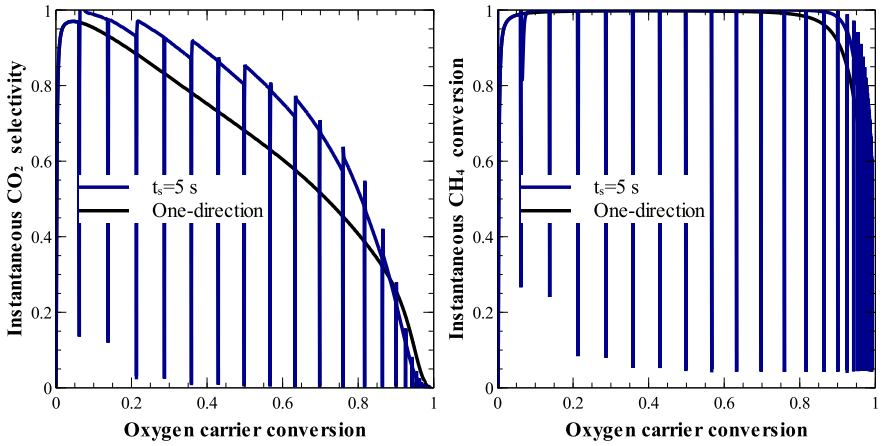

- Reactor still suboptimal
- *Performance enhancement improved*

Han L, Zhou Z, Bollas GM. Chemical-looping combustion in a reverse-flow fixed-bed reactor. Appl Energy 2014

Bollas GM, Han L. Reverse-Flow Reactor for Chemical-Looping Combustion and Reforming of Gaseous Fuels; US Provisional Patent - University of Connecticut, 2014.

Scaled-up Performance metrics II

Oxygen carrier conversion

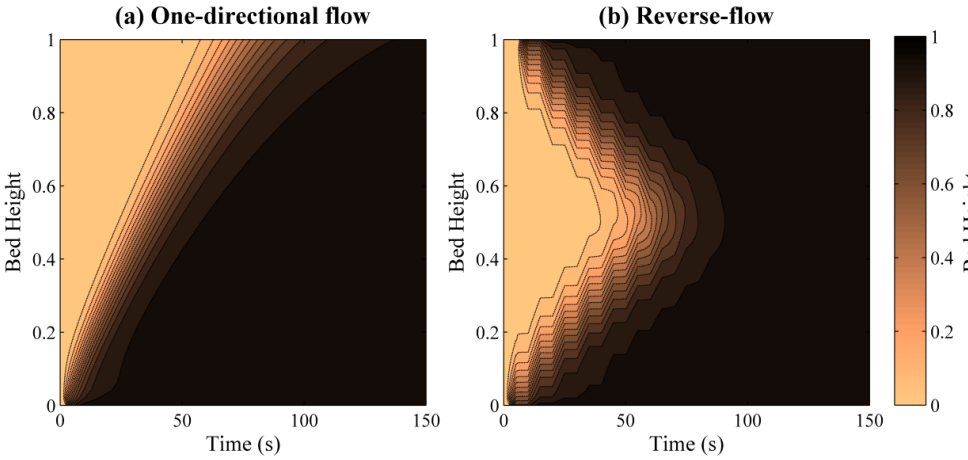

Bed Temperature Profile

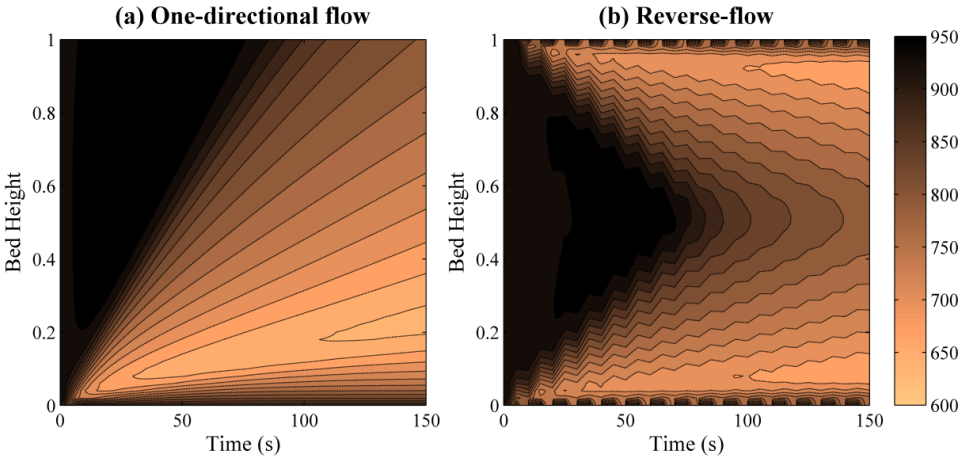

Carbon Formation

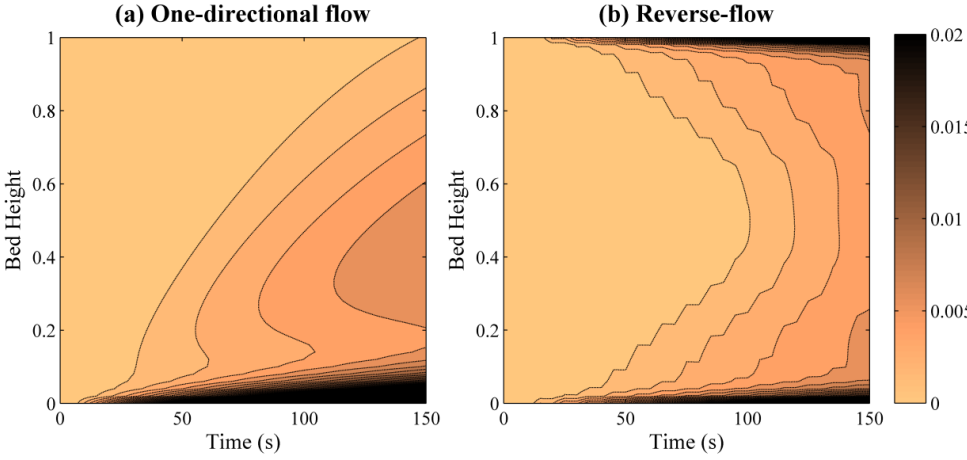

Solid Carbon selectivity and Max Bed T drop

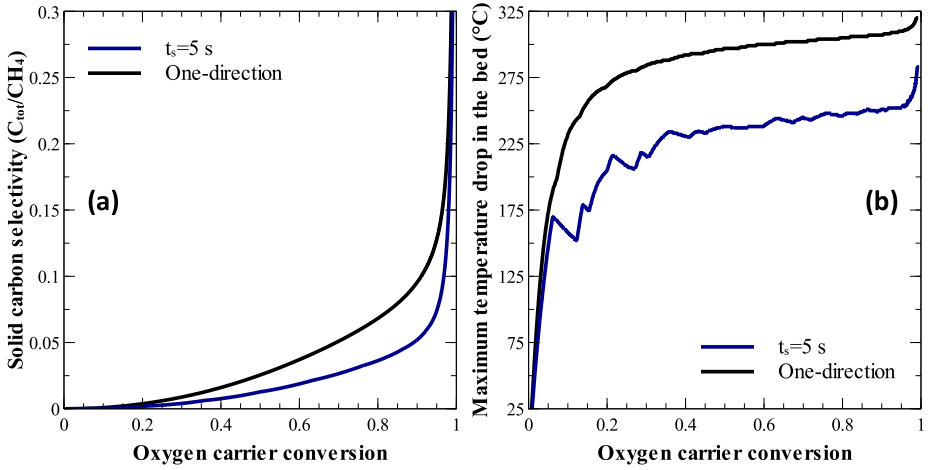

Han L, Zhou Z, Bollas GM. Chemical-looping combustion in a reverse-flow fixed-bed reactor. Applied Energy 2014

Conclusions

- What we should have done (Model-Based Development)
  - Statistical Analysis of Existing Data and Kinetics Models (F-test, AICc)
  - Fixed-bed model utilizing statistically significant kinetics
  - Optimal Experimental Design for derivation/validation of unknown kinetics
  - Fluidized-bed model prediction and validation
  - Fixed-bed / Fluidized-bed comparison
  - Reverse-flow fixed-bed reactor invention
- What we accomplished so far:
  - A novel reactor concept was invented that addresses the roadblocks to commercialization of existing chemical-looping processes
- **Our Aim**
  - *to put chemical-looping research and technology on a fundamentally new learning curve; one that relaxes the requirement for fluidized-bed reactor systems and is capable of making chemical-looping a disruptive new technology*

Acknowledgments

NSF CAREER Award
No. 1054718
Process and Reaction Engineering Program, CBET

UCONN Prototype Fund
Office of the Vice President for Research

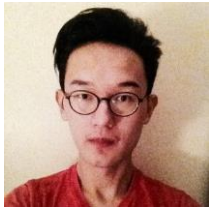

- **Zhiquan Zhou**
  4th year PhD Student, CBE UConn
  Fluidized bed modeling, dynamic parameter estimation, statistical analysis

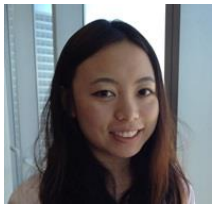

- **Lu Han**
  3rd year PhD Student, CBE UConn
  gPROMS, sensitivity analysis, optimal experimental design

- Ari Fischer
- Oscar Nordness
- Catherine Cheu
- Kyle Such
- Clarke Palmer

Thank you!

George M. Bollas

Department of Chemical & Biomolecular Engineering
University of Connecticut

http://pdsol.engr.uconn.edu